FERMILAB-TM-2582-E

LHC/Tevatron NOTE

ATLAS-CONF-2014-008
CDF Note 11071
CMS PAS TOP-13-014
D0 Note 6416

March 17, 2014

First combination of Tevatron and LHC measurements of the top-quark mass

The ATLAS, CDF, CMS and D0 Collaborations[1]

Abstract

We present a combination of measurements of the mass of the top quark, m_{top}, performed by the CDF and D0 experiments at the Tevatron collider and the ATLAS and CMS experiments at the Large Hadron Collider (LHC). The Tevatron data correspond to an integrated luminosity of up to 8.7 fb^{-1} of proton-antiproton collisions from Run II of the Tevatron at a centre-of-mass energy of 1.96 TeV. The LHC data correspond to an integrated luminosity of up to 4.9 fb^{-1} of proton-proton collisions from the run at a centre-of-mass energy of 7 TeV. The combination includes measurements in the $t\bar{t} \rightarrow$ lepton+jets, $t\bar{t} \rightarrow$ dilepton, $t\bar{t} \rightarrow$ all jets and $t\bar{t} \rightarrow E_{\mathrm{T}}^{\mathrm{miss}}$+jets final states. The resulting combined measurement of m_{top} is 173.34 ± 0.27 (stat) ± 0.71 (syst) GeV, with a total uncertainty of 0.76 GeV.

[1]Work within the Tevatron Electroweak (TEV-EW-WG) and the Top Physics LHC (TOP-LHC-WG) working groups. More information at http://tevewwg.fnal.gov and http://twiki.cern.ch/twiki/bin/view/LHCPhysics/TopLHCWG.

Operated by Fermi Research Alliance, LLC under Contract No. DE-AC02-07CH11359 with the United States Department of Energy

1 Introduction

The mass of the top quark ($m_{\rm top}$) is an important parameter of the standard model of particle physics (SM). Precise measurements of $m_{\rm top}$ provide critical inputs to fits of global electroweak parameters [1, 2] that constrain the properties of the Higgs boson, and help assess the internal consistency of the SM and of its extensions. In addition, the value of $m_{\rm top}$ affects the stability of the SM Higgs potential, which has cosmological implications [3–5].

Many measurements of $m_{\rm top}$ have been performed by the CDF and D0 collaborations based on Tevatron proton-antiproton ($p\overline{p}$) data from Run I (at a centre-of-mass energy, $\sqrt{s}$, of 1.8 TeV) and Run II ($\sqrt{s}$ = 1.96 TeV), corresponding to integrated luminosities ($\mathcal{L}_{\rm int}$) of up to 8.7 fb^{-1}. In addition, measurements of $m_{\rm top}$ from the LHC by ATLAS and CMS, based on proton-proton (pp) collisions at $\sqrt{s}$ = 7 TeV, recorded during 2010 and 2011 for integrated luminosities of up to 4.9 fb^{-1}, have become available.

The Tevatron $m_{\rm top}$ combination results in $m_{\rm top}$ = 173.20 ± 0.51 (stat) ± 0.71 (syst) GeV ≡ 173.20 ± 0.87 GeV [6]. The corresponding LHC combination yields $m_{\rm top}$ = 173.29 ± 0.23 (stat) ± 0.92 (syst) GeV ≡ 173.29 ± 0.95 GeV [7]. This analysis combines the most precise individual $m_{\rm top}$ results in each $t\bar{t}$ final state, for each collaboration, to get the best overall estimate.

This note describes the first combination of Tevatron and LHC $m_{\rm top}$ measurements, six from the Tevatron collider, based on Run II $p\overline{p}$ data collected at $\sqrt{s}$ = 1.96 TeV, and five from the LHC, based on the pp data at $\sqrt{s}$ = 7 TeV. For CDF, these measurements include the $m_{\rm top}$ results obtained for the $t\bar{t} \to$ lepton+jets, $t\bar{t} \to$ dilepton, $t\bar{t} \to$ all jets, and the $t\bar{t} \to E_{\rm T}^{\rm miss}$+jets channels[1] using up to $\mathcal{L}_{\rm int}$ = 8.7 fb^{-1} of data [8–11]. For D0, the measurements are for the $t\bar{t} \to$ lepton+jets, and $t\bar{t} \to$ dilepton channels using up to $\mathcal{L}_{\rm int}$ = 5.3 fb^{-1} of data [12, 13]. The ATLAS measurements comprise the results obtained in the $t\bar{t} \to$ lepton+jets and the $t\bar{t} \to$ dilepton channels using $\mathcal{L}_{\rm int}$ = 4.7 fb^{-1} of data [14, 15]. For CMS, the measurements, based on up to $\mathcal{L}_{\rm int}$ = 4.9 fb^{-1} of data, refer to the $t\bar{t} \to$ lepton+jets, $t\bar{t} \to$ dilepton and $t\bar{t} \to$ all jets channels [16–18]. In all measurements considered in the present combination, the analyses are calibrated to the Monte Carlo (MC) top-quark mass definition. It is expected that the difference between the MC mass definition and the formal pole mass of the top quark is up to the order of 1 GeV (see Refs. [19, 20] and references therein).

This document is organised as follows. After a brief description in Section 2 of the methodology used for the combination, an overview of the input measurements is given in Sections 3 and 4. Details of the mapping between the categories of uncertainties for CDF, D0, ATLAS and CMS, and their corresponding correlations, are described in Section 5. The results of the combination are presented in Section 6, followed in Section 7 by a discussion of their dependence on the categorisation of the uncertainties and on the assumed correlations. Finally, the summary and conclusions are given in Section 8.

2 Methodology

The combination is performed using the Best Linear Unbiased Estimate (BLUE) method [21,22], implemented as described in Ref. [23]. BLUE determines the coefficients (weights) to be used in a linear combination of the input measurements by minimising the total uncertainty of the combined result. In the algorithm, assuming that all uncertainties are distributed according to Gaussian probability density functions, both statistical and systematic uncertainties, and their correlations, are taken into account. A realistic estimate of the correlations is made and the effect of the various assumptions on the final result is evaluated.

[1] The $t\bar{t} \to$ lepton+jets, $t\bar{t} \to$ dilepton, and $t\bar{t} \to$ all jets channels correspond to the experimental final states related to the $t\bar{t}$ decays $t\bar{t} \to \bar{l}\nu b\, q\bar{q}'\bar{b}$, $t\bar{t} \to \bar{l}\nu b\, l\bar{\nu}\bar{b}$ and $t\bar{t} \to q\bar{q}'b\, q\bar{q}'\bar{b}$, respectively. The $t\bar{t} \to E_{\rm T}^{\rm miss}$+jets channel relates to the final state from $t\bar{t} \to \bar{l}\nu b\, q\bar{q}'\bar{b}$ selected using missing transverse energy signatures, $E_{\rm T}^{\rm miss}$, rather than explicit charged lepton identification criteria.

3 Measurements calibration using Monte Carlo simulation

The MC generation of signal $t\bar{t}$ and background events proceeds through the simulation of a primary hard interaction process (*e.g.*, $q\bar{q}, gg \to t\bar{t}$), accompanied by parton showers, and by non-perturbative interactions that convert the showers into colourless hadrons. In a subsequent step, soft interactions reflected in the underlying event are also included in the calculations [19]. The simulated events are processed through experiment-specific simulation and reconstruction software, and the reconstructed final state particles are clustered into jets, that can be associated with the initial partons. Within CDF, jets are reconstructed using a cone algorithm with radius parameter $R = 0.4$ [24], while D0 employs a midpoint iterative seed-based cone algorithm, with $R = 0.5$ [25]. In both cases, calorimeter information is used as input of the clustering algorithms and R is defined as $\sqrt{\Delta\eta^2 + \Delta\phi^2}$, where $\Delta\eta$ is the pseudo-rapidity and $\Delta\phi$ is the azimuthal angle of a given calorimeter energy deposit relative to the direction of the jet. Within ATLAS, starting from energy clusters of adjacent calorimeter cells called topological clusters [26–28], jets are formed using the anti-k_t algorithm [29] with a radius parameter $R = 0.4$. In CMS, events are reconstructed with the particle-flow algorithm [30] that combines the information from all CMS sub-detectors to identify and reconstruct individual objects produced in the pp collision. Particle flow objects are used as input for jet clustering also based on the anti-k_t algorithm, but with a distance parameter of $R = 0.5$ [29].

Jet energy scale (JES) calibration procedures, applied after jet reconstruction, are meant to ensure the correct measurement of the average jet energy across the whole detector, and they are designed to be independent of additional events produced in $p\overline{p}$ or pp collisions ("pile-up"[2]), especially at high luminosity regimes, compounding on the event of interest. In general, energy contributions from pile-up events are subtracted, and the jet response in different regions of the calorimeter (central-forward) is inter-calibrated. Jet energy corrections account for the energy lost in uninstrumented regions between calorimeter modules, for differences between electromagnetically and hadronically interacting particles, as well as for calorimeter module irregularities. In addition corrections for shower particles scattered in or out of the reconstructed jets are typically included. The calibration procedures use single hadron calorimeter response measurements, systematic MC simulation variations as well as in situ techniques, where the jet transverse momentum (p_{T}) is compared to the p_{T} of a reference object. CDF calibrates the jet transverse momentum using test-beam data and single-particle simulated events and corrects the jet energy to the parton level [31]. D0 determines the jet energy scale using photon+jets and dijet events and calibrates jets in data as well as in MC to the observed particle level. MC particle level jets are clustered from stable particles after fragmentation [32, 33]. Similar procedures are in place within the ATLAS and CMS collaborations [27,28,34,35]: after pile-up jet energy offset corrections, the reconstructed jet energies in MC are restored to that from stable particle jets. Residual calibrations, derived using in situ methods where the jet transverse momentum is compared to the p_T of a reference object (*e.g.* using γ/Z+jet events), are then applied to data relative to the MC.

Depending on the experiment, different MC programs and settings are used in m_{top} analyses. The baseline MC program for the simulation and calibration of the top-quark mass analyses in the CDF experiment is Pythia [36] with Tune A [37], based on CDF underlying event data. Pythia is used for the simulation of the hard process (using leading order, LO, matrix elements), the parton shower and the underlying event modelling. D0 adopts the tree-level multi-leg generator Alpgen [38] interfaced with Pythia for parton showering, using a modified version of Tune A [39]. Alpgen implements a parton-jet matching, using the MLM prescription [40], that avoids double counting of partons in the hard process and in the parton shower in overlapping regions of jet kinematics. The baseline MC program for ATLAS is Powheg interfaced with Pythia [36, 41], with the Perugia 2011C tune [42]. Powheg uses next-to-leading order (NLO) matrix element calculations interfaced with parton showers. The MadGraph tree-level multi-leg generator [43], interfaced to Pythia with the Z2 tune [44, 45], is used within CMS. Similarly to D0, the parton configurations at CMS generated with MadGraph are matched to parton showers [40]. The parton distribution functions (PDF) CTEQ5L [46], CTEQ6L1 [47], CT10 [48] and CTEQ6.6L [49] are used respectively by the CDF, D0, ATLAS and CMS collaborations as input for the matrix

[2]Pile-up is the term given to the extra signal produced in the detector by $p\overline{p}$ or pp interactions other than the primary hard scattering.

Experiment	Matrix Element	Parton shower / hadronisation	PDF	Tune
CDF	PYTHIA	PYTHIA	CTEQ5L	Tune A
D0	ALPGEN	PYTHIA	CTEQ6L1	Mod. Tune A
ATLAS	POWHEG	PYTHIA	CT10	Perugia2011C
CMS	MADGRAPH	PYTHIA	CTEQ6.6L	Z2

Table 1: Baseline $t\bar{t}$ signal MC used in $m_{\rm top}$ analyses and their main settings for the various experiments. See text for details and references.

Experiment	$t\bar{t}$ final state	$\mathcal{L}_{\rm int}$ [fb^{-1}]	$m_{\rm top}$ ± (stat.) ± (syst.) [GeV]	Total uncertainty on $m_{\rm top}$ [GeV] ([%])	Reference
CDF	l+jets	8.7	172.85 ± 0.52 ± 0.99	1.12 (0.65)	[8]
	dilepton	5.6	170.28 ± 1.95 ± 3.13	3.69 (2.17)	[9]
	all jets	5.8	172.47 ± 1.43 ± 1.41	2.01 (1.16)	[10]
	$E_{\rm T}^{\rm miss}$+jets	8.7	173.93 ± 1.26 ± 1.36	1.85 (1.07)	[11]
D0	l+jets	3.6	174.94 ± 0.83 ± 1.25	1.50 (0.86)	[12]
	dilepton	5.3	174.00 ± 2.36 ± 1.49	2.79 (1.60)	[13]
ATLAS	l+jets	4.7	172.31 ± 0.23 ± 1.53	1.55 (0.90)	[14]
	dilepton	4.7	173.09 ± 0.64 ± 1.50	1.63 (0.94)	[15]
CMS	l+jets	4.9	173.49 ± 0.27 ± 1.03	1.06 (0.61)	[16]
	dilepton	4.9	172.50 ± 0.43 ± 1.46	1.52 (0.88)	[17]
	all jets	3.5	173.49 ± 0.69 ± 1.23	1.41 (0.81)	[18]

Table 2: Overview of the 11 input measurements used in this $m_{\rm top}$ combination.

element calculations.

The baseline $t\bar{t}$ signal MC used in the $m_{\rm top}$ analyses considered here, and their main settings across the various experiments, are summarised in Table 1.

A systematic uncertainty covering differences between generator models is assigned to the input measurements, and ranges from 0.02 GeV to 0.25 GeV, depending on the analysis (typically 0.10 GeV for CDF, and 0.25 GeV for D0 measurements; 0.20 GeV for ATLAS, and in the range [0.02, 0.19] GeV for CMS inputs). This is included together with other effects in the signal modelling systematic uncertainty (labelled MC in Section 5) described below. The systematic uncertainty related to the specific MC choice is found to be marginal with respect to the possible intrinsic difference between the top-quark mass implemented in any MC and the pole mass definition [19].

4 Input measurements

This $m_{\rm top}$ combination takes as inputs all of the measurements from the previous LHC combination [7], and a partial set of those from the latest Tevatron combination [6]. The chosen inputs correspond to the best measurements per channel and per experiment (excluding results from Tevatron Run I). These comprise (i) four CDF published results from the $t\bar{t} \to$ lepton+jets, $t\bar{t} \to$ dilepton, $t\bar{t} \to$ all jets, and $t\bar{t} \to E_{\rm T}^{\rm miss}$+jets channels [8–11], (ii) two D0 published measurements from the $t\bar{t} \to$ lepton+jets, and $t\bar{t} \to$ dilepton channels [12, 13], (iii) two preliminary ATLAS results in the $t\bar{t} \to$ lepton+jets and $t\bar{t} \to$ dilepton channels [14, 15], and (iv) three published results from the CMS collaboration in the $t\bar{t} \to$ lepton+jets, $t\bar{t} \to$ dilepton, and $t\bar{t} \to$ all jets channels [16–18].

An overview of the input $m_{\rm top}$ measurements used in this combination is shown in Table 2. Further details are provided in the following sections.

4.1 CDF measurements

The CDF measurements in the $t\bar{t} \to$ lepton+jets and $t\bar{t} \to E_{\mathrm{T}}^{\mathrm{miss}}$+jets channels are based on the full Run II data set of 8.7 fb^{-1} [8, 11]. The m_{top} results in the $t\bar{t} \to$ dilepton and $t\bar{t} \to$ all jets channels use 5.6 fb^{-1} and 5.8 fb^{-1} of data, respectively [9, 10]. The CDF Run I measurements have relatively large uncertainties and for simplicity are thus not considered in this combination. The CDF analyses based upon charged particle tracking that use the transverse decay length of b-tagged jets (L_{xy}) or the transverse momentum of electrons and muons from W boson decays ($p_{\mathrm{T}}^{\mathrm{lep}}$) use only part of the available Run II data [50, 51]. Due to their large total uncertainties and statistical correlation with $t\bar{t} \to$ lepton+jets and $t\bar{t} \to$ dilepton events, these results are not included in this combination.

In all four CDF analyses, the template method is used, and the event reconstruction is based on a kinematic fit to the $t\bar{t}$ decay hypothesis. For example, the templates may be the top-quark mass reconstructed from a kinematic fit in MC samples, generated using different input m_{top}. The templates are transformed to continuous functions of m_{top}, either through a non-parametric kernel-density estimator [52], or by fitting an analytic function that interpolates between the discrete input values of m_{top}. These are then used in a maximum likelihood fit to the data.

The analysis in the $t\bar{t} \to$ dilepton channel measures m_{top} using the "neutrino weighting" algorithm [53, 54]. This procedure steps through different hypotheses for the pseudo-rapidity distributions of the two neutrinos in the final state. For each hypothesis, the algorithm calculates the full event kinematics and assigns a weight to the resulting reconstructed top-quark mass based on the agreement between the calculated and measured missing transverse energy. The solution corresponding to the maximum weight is selected to represent the event. The analysis also uses template distributions of m_{T2}, a variable related to the transverse masses of the top quarks [9].

In the case of the $t\bar{t} \to$ lepton+jets, $t\bar{t} \to$ all jets, and $t\bar{t} \to E_{\mathrm{T}}^{\mathrm{miss}}$+jets channels, two- or three-dimensional template fits (depending on the number of input template distributions utilised) are performed to determine m_{top} along with a global jet-energy scale factor JSF (denoted as "JES" in the original publications). The JSF is constrained by the response of light-quark jets by the kinematic information in $W \to q\bar{q}'$ decays (referred to as in situ $t\bar{t}$ jet energy calibration). This technique was pioneered in the $t\bar{t} \to$ lepton+jets analyses by CDF and D0 at the beginning of Run II of the Tevatron [55, 56]. In the fitting procedures, the external information about the uncertainty on the JES is used as a prior in determining the JSF. The resulting correlation among different CDF measurements and categories of uncertainty is evaluated by comparing the m_{top} values both with and without the JES priors, and found to be negligible. The jet energy calibrations for the $t\bar{t} \to$ lepton+jets analysis are improved using an artificial neural network to achieve a better b-jet energy resolution. In a way similar to what is described in Ref. [57], this algorithm incorporates precision tracking and secondary vertex information, in addition to standard calorimeter measurements.

4.2 D0 measurements

The two D0 measurements of m_{top} used in this combination correspond to the best D0 measurements in the $t\bar{t} \to$ lepton+jets and $t\bar{t} \to$ dilepton channels [12, 13]. D0 results from Run I also have relatively large uncertainties, and for simplicity are thus not used in this combination. The $t\bar{t} \to$ lepton+jets measurement is based on 3.6 fb^{-1} of Run II Tevatron data [12]. It uses a matrix element method [58] with an in situ jet energy calibration. To optimise the precision, it incorporates the constraint from the invariant mass of the hadronically decaying W boson from the top quark ($t \to Wb$), together with an external prior on the jet energy calibrated through studies of exclusive γ+jet and jet events. A flavor-dependent jet response correction is further applied to MC events [33]. The result using 2.6 fb^{-1} [12] of data is combined with the 1 fb^{-1} measurement [59] which uses statistically independent data. To take into account correlations among different sources of systematic uncertainty, the contribution from the JES prior is kept separate following the procedure detailed in Ref. [60].

The $t\bar{t} \to$ dilepton measurement is based on 5.3 fb^{-1} of Run II Tevatron data [13]. The measurement

uses the neutrino weighting technique, as described for the corresponding CDF analysis. In addition, the JSF re-calibration from the $t\bar{t} \rightarrow$ lepton+jets analysis is applied to this channel, along with an estimate of the uncertainty in transferring that calibration to the dilepton event topology. The result using 4.3 fb^{-1} [13] of data is combined with the 1 fb^{-1} measurement [61]. As in the case of the $t\bar{t} \rightarrow$ lepton+jets result, these analyses use statistically independent data.

4.3 ATLAS measurements

All the ATLAS measurements of m_{top} rely on the template method, and use analytic probability density functions for interpolation.

In the $t\bar{t} \rightarrow$ lepton+jets analysis, events are reconstructed using a kinematic fit to the $t\bar{t}$ decay hypothesis ($t\bar{t} \rightarrow \bar{l}\nu b\, q\bar{q}'\bar{b}$). A three-dimensional template method is used, where m_{top} is determined simultaneously with a JSF from $W \rightarrow q\bar{q}'$ decays and a separate b-to-light-quark energy scale factor (bJSF) [14]. The JSF and bJSF account for differences between data and simulation in the light-quark and in the relative b- and light-quark jet energy scale, respectively, thereby mitigating the corresponding systematic uncertainties. No prior knowledge of the uncertainty related to the light- and b-quark jet energy scales is used when determining the JSF and the bJSF parameters.

The $t\bar{t} \rightarrow$ dilepton analysis is based on a one-dimensional template method, where the templates are constructed for the m_{lb} observable, defined as the per-event average invariant mass of the two lepton (either electron or muon) plus b-jet pairs in each event from the decay of the top quarks [15].

4.4 CMS measurements

The CMS input measurements in the $t\bar{t} \rightarrow$ lepton+jets [16] and $t\bar{t} \rightarrow$ all jets [18] channels are based on the ideogram method [62], and employ a kinematic fit of the decay products to a $t\bar{t}$ hypothesis ($t\bar{t} \rightarrow \bar{l}\nu b\, q\bar{q}'\bar{b}$ or $t\bar{t} \rightarrow q\bar{q}'b\, q\bar{q}'\bar{b}$). MC-based likelihood functions are exploited for each event (ideograms) that depend only on the top-quark mass or on both m_{top} and a JSF. The ideograms reflect the compatibility of the kinematics of the event with a given decay hypothesis. For the $t\bar{t} \rightarrow$ lepton+jets analysis m_{top} is derived simultaneously with a JSF from $t \rightarrow Wb$ ($W \rightarrow q\bar{q}'$) decays (two-dimensional ideogram method); whereas for the $t\bar{t} \rightarrow$ all jets analysis only m_{top} is extracted from a fit to the data (one-dimensional ideogram method). Similar to the ATLAS $t\bar{t} \rightarrow$ lepton+jets analysis, no prior knowledge of the uncertainty on the jet energy scale is used to determine the JSF.

For the CMS $t\bar{t} \rightarrow$ dilepton analysis, m_{top} is obtained from an analytical matrix-weighting technique, where the full reconstruction of the event kinematics is done under different m_{top} assumptions. For each event, the most likely m_{top} hypothesis, fulfilling $t\bar{t}$ kinematic constraints, is obtained by assigning weights that are based on probability density functions for the energy of the charged lepton taken from simulation, whic are applied in the solution of the kinematic equations [17].

Results from alternative techniques [63, 64], characterised by different sensitivities to the dominant systematic contributions, have recently become available but are not included in the present analysis.

5 Evaluation and categorisation of uncertainties

In addition to the statistical uncertainty, the measurements of m_{top} are subject to several sources of systematic effects. These are subdivided using the following categories, that are detailed in Sections 5.2, 5.3 and 5.4.

- **JES:** this group of uncertainties stems from the limited understanding of the detector response to (and the modelling of) different types of jets (b-quark, light-quark or gluon originated jets).
- **Theory and modelling:** this class of uncertainties is related to the MC modelling of the $t\bar{t}$ signal, and arises from several components. These range from the specific choice of the MC generator and the

associated PDF, to the models used for the parton hadronisation, the underlying event, and the colour reconnection effects. In addition, variations of the settings used to regulate the QCD radiation accompanying the $t\bar{t}$ production are considered.

- **Detector modelling, background contamination, environment:** these categories comprise systematic uncertainties stemming from detector resolution effects, reconstruction efficiencies, and the b-tagging performance in data relative to the MC. In addition, effects related to normalisation and differential distributions of backgrounds events, and the modelling of the data-taking conditions in the MC simulation relative to the data, are included in this category.

Systematic uncertainties on all eleven m_{top} input values are evaluated by changing the respective quantities by ± 1 standard deviation, or by changing the $t\bar{t}$ signal modelling parameters relative to the default analysis. For each component of uncertainty, the observed shift in m_{top} relative to the nominal analysis is used to determine the corresponding top-quark mass uncertainty. The total uncertainty is defined by the quadratic sum of all individual contributions, *i.e.* neglecting possible correlations among different uncertainty classes (by construction expected to be minimal), as well as non-linear effects on the measured value of m_{top}.

Depending on the methods and experimental details, different correlations can arise among the sources of uncertainty of the eleven input m_{top} measurements. The following details how these are treated in the evaluation of the final results.

The CDF and D0 categorisations of uncertainties, and their assumed correlations, are documented in Refs. [6,39]. The categorisations for ATLAS and CMS closely follow those of Ref. [7] (see Appendix A for details on naming conventions). In certain cases, without altering the total uncertainty of the input measurements, the breakdowns into categories of systematic uncertainties differ from the original publications[3]. The latter typically have a coarser categorisation and modifications were required to match the desired uncertainty classes. The correlation coefficients ρ_{CDF}, ρ_{D0}, ρ_{ATL}, and ρ_{CMS} indicate the assumed correlation among measurements within the same experiment (collectively referred to as ρ_{EXP}), while ρ_{LHC} and ρ_{TEV} indicate the correlation assumed between measurements at the LHC and the Tevatron analyses. Correlation coefficients $\rho_{\text{ATL-TEV}}$ and $\rho_{\text{CMS-TEV}}$ stand for the correlations between measurements from ATLAS or CMS and the Tevatron (ρ_{COL} as a short hand notation), respectively.

Specific systematic uncertainties on individual m_{top} inputs, stemming from modelling of production processes, detector response and other effects, can differ for many reasons. Analysis-specific issues, such as the amount of kinematic information exploited in the analysis, and the level of sophistication of the $t\bar{t}$ reconstruction algorithms, can influence the sensitivity of the input measurements to different $t\bar{t}$ modelling systematic uncertainties. Similarly, differences in analysis methods, for example the possibility to simultaneously determine global jet energy scale factors and m_{top}, can lead to a mitigation of the JES-related systematic uncertainties. This can reduce certain signal modelling systematics, but possibly increase some detector related uncertainties. Finally, detector performance can be affected by experimental specifications. For example, the dependence of the JES uncertainty on jet p_{T} can affect the contribution of the JES component to the uncertainty on m_{top}, for different cutoffs on p_{T}, even for analyses implementing in situ $t \to Wb$, $W \to q\bar{q}'$ calibrations.

The uncertainties and the assumed correlations among classes are summarised in Tables 3 and 4, respectively, and detailed below. These reflect the present understanding and the limitations originating from independent paths followed by the experiments to evaluate the individual sources of uncertainty. The stability of the result under different assumptions is discussed in Section 7.

5.1 Statistical uncertainty

Stat: This is the statistical uncertainty associated with the m_{top} determination from the available data. It is uncorrelated between different $t\bar{t}$ final states, experiments and the two colliders (orthogonal data samples).

[3] When asymmetric uncertainties were reported [17], a symmetrisation procedure is applied taking the maximum between the absolute values of the positive and negative uncertainties.

	Input measurements and uncertainties in GeV											
	CDF				D0		ATLAS		CMS			World
Uncertainty	l+jets	di-l	all jets	$E_{\mathrm{T}}^{\mathrm{miss}}$	l+jets	di-l	l+jets	di-l	l+jets	di-l	all jets	Combination
m_{top}	172.85	170.28	172.47	173.93	174.94	174.00	172.31	173.09	173.49	172.50	173.49	173.34
Stat	0.52	1.95	1.43	1.26	0.83	2.36	0.23	0.64	0.27	0.43	0.69	0.27
iJES	0.49	n.a.	0.95	1.05	0.47	0.55	0.72	n.a.	0.33	n.a.	n.a.	0.24
stdJES	0.53	2.99	0.45	0.44	0.63	0.56	0.70	0.89	0.24	0.78	0.78	0.20
flavourJES	0.09	0.14	0.03	0.10	0.26	0.40	0.36	0.02	0.11	0.58	0.58	0.12
bJES	0.16	0.33	0.15	0.17	0.07	0.20	0.08	0.71	0.61	0.76	0.49	0.25
MC	0.56	0.36	0.49	0.48	0.63	0.50	0.35	0.64	0.15	0.06	0.28	0.38
Rad	0.06	0.22	0.10	0.28	0.26	0.30	0.45	0.37	0.30	0.58	0.33	0.21
CR	0.21	0.51	0.32	0.28	0.28	0.55	0.32	0.29	0.54	0.13	0.15	0.31
PDF	0.08	0.31	0.19	0.16	0.21	0.30	0.17	0.12	0.07	0.09	0.06	0.09
DetMod	<0.01	<0.01	<0.01	<0.01	0.36	0.50	0.23	0.22	0.24	0.18	0.28	0.10
b-tag	0.03	n.e.	0.10	n.e.	0.10	<0.01	0.81	0.46	0.12	0.09	0.06	0.11
LepPt	0.03	0.27	n.a.	n.a.	0.18	0.35	0.04	0.12	0.02	0.14	n.a.	0.02
BGMC	0.12	0.24	n.a.	n.a.	0.18	n.a.	n.a.	0.14	0.13	0.05	n.a.	0.10
BGData	0.16	0.14	0.56	0.15	0.21	0.20	0.10	n.a.	n.a.	n.a.	0.13	0.07
Meth	0.05	0.12	0.38	0.21	0.16	0.51	0.13	0.07	0.06	0.40	0.13	0.05
MHI	0.07	0.23	0.08	0.18	0.05	<0.01	0.03	0.01	0.07	0.11	0.06	0.04
Total Syst	0.99	3.13	1.41	1.36	1.25	1.49	1.53	1.50	1.03	1.46	1.23	0.71
Total	1.12	3.69	2.01	1.85	1.50	2.79	1.55	1.63	1.06	1.52	1.41	0.76

Table 3: Uncertainty categories assignment for the input measurements and the result of the world m_{top} combination. All values are in GeV. In the table, "n.a." stands for not applicable; "n.e." refers to uncertainties not evaluated (see text for details).

	ρ_{EXP}				ρ_{LHC}	ρ_{TEV}	ρ_{COL}	
	ρ_{CDF}	ρ_{D0}	ρ_{ATL}	ρ_{CMS}			$\rho_{\mathrm{ATL-TEV}}$	$\rho_{\mathrm{CMS-TEV}}$
Stat	0.0	0.0	0.0	0.0	0.0	0.0	0.0	0.0
iJES	0.0	1.0	0.0	0.0	0.0	0.0	0.0	0.0
stdJES	1.0	1.0	1.0	1.0	0.0	0.0	0.0	0.0
flavourJES	1.0	1.0	1.0	1.0	0.0	0.0	0.0	0.0
bJES	1.0	1.0	1.0	1.0	0.5	1.0	1.0	0.5
MC	1.0	1.0	1.0	1.0	1.0	1.0	1.0	1.0
Rad	1.0	1.0	1.0	1.0	1.0	1.0	0.5	0.5
CR	1.0	1.0	1.0	1.0	1.0	1.0	1.0	1.0
PDF	1.0	1.0	1.0	1.0	1.0	1.0	0.5	0.5
DetMod	1.0	1.0	1.0	1.0	0.0	0.0	0.0	0.0
b-tag	1.0	1.0	1.0	1.0	0.0	0.0	0.0	0.0
LepPt	1.0	1.0	1.0	1.0	0.0	0.0	0.0	0.0
BGMC†	1.0	1.0	1.0	1.0	1.0	1.0	1.0	1.0
BGData	0.0	0.0	0.0	0.0	0.0	0.0	0.0	0.0
Meth	0.0	0.0	0.0	0.0	0.0	0.0	0.0	0.0
MHI	1.0	1.0	1.0	1.0	1.0	0.0	0.0	0.0

Table 4: Assumed correlation coefficients for each source of uncertainty. The symbols ρ_{CDF}, ρ_{D0}, ρ_{ATL}, and ρ_{CMS} represent the assumed correlations among measurements from the same experiment, while ρ_{LHC} and ρ_{TEV} indicate the correlations assumed respectively between measurements at the LHC and at the Tevatron. The $\rho_{\mathrm{ATL-TEV}}$ and $\rho_{\mathrm{CMS-TEV}}$ reflect the correlations between measurements from ATLAS or CMS and the Tevatron.
† For the BGMC, the 100% correlation is assumed only for measurements using the same $t\bar{t}$ final state.

5.2 JES uncertainties

The following systematic uncertainties stem from the limited knowledge of the JES [27, 28, 31–35, 65]. Since the methodologies and assumptions to derive JES corrections and their corresponding uncertainties are not always directly comparable between experiments, variations of the correlation assumptions described below

are considered in checking the stability of the combination (see Section 7).

iJES: This is the part of the JES uncertainty of the $m_{\rm top}$ measurements that originates from in situ $t\bar{t}$ ($t \to Wb, W \to q\bar{q}'$) calibration procedures. Being statistical in nature, it is uncorrelated among the individual measurements. For analyses performing an in situ jet calibration based on the simultaneous fit of the reconstructed W boson and top quark invariant masses, this corresponds to the additional statistical uncertainty associated with the simultaneous determination of a JSF using the $W \to q\bar{q}'$ invariant mass and $m_{\rm top}$ [8, 10–12, 14, 16]. For the ATLAS $t\bar{t} \to$ lepton+jets measurement [14], it also includes the extra statistical component due to the simultaneous determination of a bJSF. For this category, we assume that uncertainties are uncorrelated ($\rho_{\rm CDF} = \rho_{\rm ATL} = \rho_{\rm CMS} = 0$), except for the D0 $t\bar{t} \to$ lepton+jets and $t\bar{t} \to$ dilepton measurements, where the result for the JSF from the $t\bar{t} \to$ lepton+jets measurement is used to constrain the JES in the $t\bar{t} \to$ dilepton analysis ($\rho_{\rm D0} = 1$).

stdJES: (Standard light jet energy scale uncertainty, dJES in Refs. [6, 7]) This refers to the standard, non-flavour specific, part of the JES uncertainty. It is assumed to be correlated between the measurements in the same experiment but not correlated between experiments nor across colliders ($\rho_{\rm EXP} = 1, \rho_{\rm LHC} = \rho_{\rm TEV} = 0$ and $\rho_{\rm COL} \equiv \rho_{\rm ATL-TEV} = \rho_{\rm CMS-TEV} = 0$).

For CDF, this includes uncertainties on the relative jet energy correction as a function of jet η. This is evaluated using dijet data, along with Pythia and Herwig [66] simulated dijet samples [31]. In addition, uncertainties originating from the attempt to correct the jet energy to the parton level are included in this category for all CDF measurements. These are related to the out-of-cone showering corrections to the MC showers (cJES in Ref. [6]), the absolute calibration, and the modelling of the multiple hadronic interaction and the underlying events (rJES in Ref. [6]).

For D0, this uncertainty term represents almost all parts of JES calibrations. The absolute energy scale for jets in data is calibrated using γ+jet data using the "$\not\!\!E_{\rm T}^{\rm miss}$ projection fraction" method [32]. Simulated samples of γ+jets and Z+jets events are compared to data, and used to derive jet energy scale corrections for MC and data events. The JES is also corrected as a function of η for forward jets relative to the central jets using γ+jets and dijets data. Out-of-cone particle scattering corrections are determined with γ+jets simulated events.

For LHC experiments, the stdJES uncertainty category comprises three components (uncorrJES, insituγ/Z JES, and intercalibJES) [7], which in the present analysis are summed in quadrature. These are assumed to be fully correlated between measurements from the same experiment, but uncorrelated across ATLAS and CMS ($\rho_{\rm ATL} = \rho_{\rm CMS} = 1$, and $\rho_{\rm LHC} = 0$).

uncorrJES: (LHC only, part of stdJES) For ATLAS this includes contributions from the limited data sample statistics used to derive the standard jet energy calibrations. In addition, uncertainty contributions from detector-specific components, pile-up suppression techniques, and the presence of close-by jet activity are included in this source. For CMS, this uncertainty source includes the statistical uncertainty of the standard jet energy calibration, contributions stemming from the jet energy correction due to pile-up effects, uncertainties due to the variations of the calorimeter response versus time, and detector specific effects.

insituγ/ZJES: (LHC only, part of stdJES) This corresponds to the part of the JES uncertainty stemming from modelling uncertainties affecting the JES determination using γ/Z+jets events, not included in the uncorrJES category.

intercalibJES: (LHC only, part of stdJES) This is the JES uncertainty component originating from the relative jet η (central-forward) and $p_{\rm T}$ inter-calibration procedures. Within CMS, when evaluating this uncertainty contribution, an extrapolation to zero radiation is performed, and sizable statistical contributions are present[4].

[4]For the sake of simplicity and opposite to what was done in Ref. [7], the combination is carried out with $\rho_{\rm ATL} = \rho_{\rm CMS} = 1$; $\rho_{\rm LHC} = 0$.

flavourJES: This includes the part of the JES uncertainty stemming from differences in the jet energy response for various jet flavours (quark- versus gluon-originated jets) and variations of the flavour mixture with respect to that used in the calibration procedures. Contributions due to the modelling of b-quark jets are treated separately and discussed below. The combined m_{top} result is obtained with $\rho_{\mathrm{EXP}} = 1$; $\rho_{\mathrm{TEV}} = \rho_{\mathrm{LHC}} = \rho_{\mathrm{COL}} = 0$.

bJES: This accounts for an additional b-jet specific uncertainty, arising from the uncertainty in the modelling of the response of jets originating from b-quarks [34, 39, 65].

In CDF and D0, this category covers the uncertainty on the semileptonic branching fraction ($10.69 \pm 0.22) \times 10^{-2}$ [67] of B hadrons. Both collaborations re-weight $t\bar{t}$ events by the uncertainty on the central value ($\pm 2.1\%$), and take half of the resulting mass difference as the uncertainty on m_{top}. In addition, this category covers the uncertainty on the b-jet fragmentation. CDF uses the default Pythia model of b-jet fragmentation based on the Bowler model [68]. D0 uses a model with the b-fragmentation parameters tuned to data from ALEPH, DELPHI, and OPAL [69–73]. To estimate the uncertainty from different b-fragmentation models, CDF compares its m_{top} values using the fragmentation models with the LEP parameters [70–72] used by D0 to those using the parameters from the SLD experiment at SLC [73]. D0 compares the measured m_{top} with the LEP parameters to the one using parameters from SLD.

In ATLAS, this uncertainty covers the effects stemming from b-quark fragmentation, hadronisation and underlying soft radiation. It is determined using different Monte Carlo generators as well as variations of the b-quark fragmentation model [65]. For the ATLAS $t\bar{t} \rightarrow$ lepton+jets input measurement [14], due to the simultaneous fit of m_{top} together with JSF and bJSF, the impact of this uncertainty is reduced to 0.08 GeV, albeit at the cost of an additional statistical component in the iJES class, which, with the present integrated luminosity, amounts to 0.67 GeV. For CMS, the bJES uncertainty on m_{top} is evaluated applying the full flavour-dependent JES uncertainty, based on the difference in the response between light quark and gluon originated jets [34], to b-quark originated jets.

This uncertainty class is assumed to be fully correlated between measurements from the same experiments ($\rho_{\mathrm{EXP}} = 1$). It is fully correlated between the Tevatron experiments ($\rho_{\mathrm{TEV}} = 1.0$) and partially correlated across LHC experiments ($\rho_{\mathrm{LHC}} = 0.5$ assumed) because of the different methods used to evaluate it. Owing to the methodologies exploited for the estimate of this uncertainty source, different correlation assumptions are used as the baseline across experiments and colliders: $\rho_{\mathrm{ATL-TEV}} = 1$, $\rho_{\mathrm{CMS-TEV}} = 0.5$. Stability checks are performed changing the value of ρ_{LHC} and $\rho_{\mathrm{CMS-TEV}} = 0.5$ to unity (see Section 7).

5.3 Theory and modelling uncertainties

The component of the systematic uncertainty stemming from the modelling of $t\bar{t}$ signal events is divided into several sub-categories. Although different baseline MC generators and parameter settings are used within the four collaborations (Section 3 and Table 1), as default assumption, and unless otherwise stated, these uncertainty categories are assumed to be fully correlated among measurements in each experiment ($\rho_{\mathrm{exp}} = 1$), and across experiments and colliders ($\rho_{\mathrm{TEV}} = \rho_{\mathrm{LHC}} = \rho_{\mathrm{COL}} = 1$). Changes in these assumptions are considered in the combination stability checks (see Section 7).

MC: (Monte Carlo) This sub-category includes uncertainties stemming from the specific choice of the Monte Carlo generator, and the hadronisation and underlying event models. When appropriate, identical sets of hard-scatter events are used in the comparison of different MC models.

For CDF, the hadronisation and underlying event (UE) uncertainty is calculated by comparing m_{top} obtained using Pythia with Tune A of the underlying event model to results from Herwig with a tuned implementation of the underlying-event generator Jimmy [74, 75]. D0 estimates this uncertainty component by comparing m_{top} results using Alpgen interfaced to Herwig relative to the baseline Alpgen+Pythia, with the corresponding tunes. Furthermore, for both CDF and D0 measurements, a contribution to this

uncertainty category stems from higher order corrections, and the simulation of decay widths effects for the top quark and the W bosons. This is obtained by comparing $m_{\rm top}$ results from LO and NLO generators, using Pythia (CDF) or Alpgen (D0) versus MC@NLO [76, 77], and varying the relative fraction of $q\bar{q} \to t\bar{t}$ and $gg \to t\bar{t}$ sub-processes in the simulation (for CDF, a re-weighting of the gluon fusion fraction in the Pythia model from 5% to 20% is performed).

ATLAS estimates the MC generator systematic uncertainty by comparing $m_{\rm top}$ results obtained with MC@NLO with those from Powheg, both interfaced to Herwig. In addition, contributions due to the choice of the hadronisation model (Pythia versus Herwig) used in the simulation are also included (see also Section 7). For CMS, the baseline MadGraph MC setup does not include the simulation of the decay widths of the top quarks and the W bosons. A systematic uncertainty is obtained by comparing the $m_{\rm top}$ results in MC samples generated with Powheg or MadGraph to also cover this effect [7]. Both LHC experiments evaluate separately the UE contribution by comparing simulated samples interfaced to Pythia with tunes Perugia 2011 and Perugia 2011 mpiHi [42]. The UE-specific uncertainty for ATLAS and CMS measurements (separated in Ref. [7]) is added to this category.

Rad: (Radiation) This category includes uncertainties due to the modelling of QCD radiation in $t\bar{t}$ events.

Uncertainties from QCD initial state radiation are assessed by both Tevatron collaborations using a CDF measurement [78] in Drell-Yan dilepton events that have the same $q\bar{q}$ initial state as most $t\bar{t}$ events, but no final state radiation. The mean $p_{\rm T}$ of the dilepton pairs is measured as a function of the dilepton invariant mass, and the values of $\Lambda_{\rm QCD}$ and the Q^2 scale in the simulation (based on the Pythia parton shower model) that bracket the data when extrapolated to the $t\bar{t}$ mass region are found. These are used to define the corresponding parameter variations. The same variations of $\Lambda_{\rm QCD}$ and Q^2 scale are used to estimate the effect of final state radiation.

For the ATLAS measurements, variations of the initial and final state radiation (ISR/FSR) parameters within Pythia, which are constrained by $t\bar{t}$-enriched ATLAS data [79], are used to evaluate these $m_{\rm top}$ systematic uncertainties. In CMS, MadGraph MC samples with varied factorisation and renormalisation scales, as well as with varied $p_{\rm T}$ thresholds for the MLM matching [40], are used to address these systematic uncertainties. Investigations from Refs. [79–81] indicate that the ATLAS and CMS approaches describe, to a large extent, the same physics effect.

Due to the difference between the dominant initial state production processes yielding the $t\bar{t}$ pairs at the Tevatron and at the LHC, and owing to the different methods applied to constrain the radiation related parameters in the MC[5], this uncertainty contribution is assumed to be partially correlated between measurements from different colliders ($\rho_{\rm COL} \equiv \rho_{\rm ATL-TEV} = \rho_{\rm CMS-TEV} = 0.5$). Variations of these assumptions are reported in Section 7.

Some level of double counting between this uncertainty source and the stdJES and MC categories described above might be present.

CR: (Colour Reconnection) This is the part of the uncertainty related to the modelling of colour reconnection effects [82].

This uncertainty is evaluated by comparing $m_{\rm top}$ results obtained in simulated samples with the hadronisation based on Pythia tunes APro and ACRPro (for CDF and D0) [83], or Perugia 2011 and Perugia 2011 noCR (for ATLAS and CMS) [42].

PDF: (Parton Distribution Functions) This is the part of the modelling uncertainty related to the proton PDF.

[5]The Drell-Yan events used at the Tevatron mainly constrain gluon radiation off of (anti)quarks. On the other hand, the $t\bar{t}$ dilepton topologies, used in the jet-veto analyses [79, 81] at the LHC, mainly constrain QCD radiation off of gluons.

For CDF, the uncertainty is evaluated by comparing CTEQ5L [46] results with MRST98L [84], by changing the value of the strong coupling constant, α_S, in the MRST98L model, and by re-weighting the simulated events according to the 20 eigenvector variations in CTEQ6M [47]. D0 estimates this uncertainty by re-weighting the Pythia model to match possible excursions in the parameters represented by the 20 CTEQ6M eigenvector variations.

For ATLAS and CMS, the PDF uncertainty is evaluated by re-weighting the simulated signal events according to the ratio of the default central PDF (CT10 and CTEQ6.6L for ATLAS and CMS, respectively) and the corresponding eigenvector variations [48, 49, 85]. The uncertainty contribution corresponding to the re-weighting of the events to alternative PDF sets is found to be smaller than the above variation and not included.

Using the methodology described in Ref. [86], the correlation of the effects due to PDF variations on $t\bar{t}$ production mechanisms between the Tevatron and the LHC is estimated to be moderate (about 50 – 60% for the LHC run at $\sqrt{s} = 7$ TeV) and to decrease as a function of the LHC centre-of-mass energy. While this result could be applied for the $m_{\rm top}$ determinations using $t\bar{t}$ production cross section measurements, the correlation of the uncertainties due to PDF, across the input measurements considered here, might be reduced owing to the $t\bar{t}$ event reconstruction. As a result, $\rho_{\rm COL} = 0.5$ is used as the default correlation assumption. Variations of these assumptions are reported in Section 7.

5.4 Uncertainties on the detector modelling, background contamination, and environment

The following systematic uncertainties arise from effects not directly connected to the JES and the theoretical modelling of the $t\bar{t}$ signal.

DetMod: (Detector Modelling) This category relates to uncertainties in the modelling of detector effects (uncertainties related to the b-jet and lepton identification are treated separately as detailed below). For Tevatron experiments, this systematic uncertainty arises from uncertainties in the modelling of the detector in the MC simulation. For D0, this includes the uncertainties from jet resolution and jet reconstruction [33]. At CDF, the jet reconstruction efficiency and resolution in the MC closely match those in data [31]. The small differences propagated to $m_{\rm top}$, after increasing the jet resolution in the MC by $\approx 4\%$ in absolute value, lead to a negligible uncertainty (<0.01 GeV). For LHC experiments, this category includes uncertainties in the jet energy resolution [34, 87], the jet reconstruction efficiency [27] as well as uncertainties related to the reconstruction of the missing transverse energy, $E_{\rm T}^{\rm miss}$ [88, 89]. This uncertainty class is assumed to be fully correlated between measurements from the same experiments ($\rho_{\rm EXP} = 1$), but uncorrelated across experiments ($\rho_{\rm TEV} = \rho_{\rm LHC} = \rho_{\rm COL} = 0$).

b-tag: (b-tagging) This is the part of the uncertainty related to the modelling of the b-tagging efficiency and the light-quark jet rejection factors in the MC simulation with respect to the data [39, 90–95].

CDF reports that any difference between the b-tagging behaviour in MC and data [90] has a marginal impact on the measurement of $m_{\rm top}$: the latest CDF measurements in the $t\bar{t} \to$ lepton+jets and $t\bar{t} \to$ all jets channels estimated this effect to be 0.03 GeV and 0.1 GeV, respectively. It is not evaluated for the $t\bar{t} \to$ dilepton and $t\bar{t} \to E_{\rm T}^{\rm miss}$+jets results ("n.e." in Table 3). D0 also exploits b-tagging algorithms in the analyses [95]: the b-tagging efficiency for simulated events is adjusted to match the data, and the corresponding uncertainties are propagated to the $m_{\rm top}$ analyses. The $m_{\rm top}$ combined result is obtained with $\rho_{\rm EXP} = 1$ and $\rho_{\rm TEV} = 0$.

For LHC experiments, data-to-MC b-tagging scale factors (SF) are derived as a function of the jet properties (flavour, $p_{\rm T}$, and η) using b/c/light-quark enriched dijet data samples. In some cases (ATLAS l+jets analysis) SF are derived from a combination of different calibrations obtained from a $t\bar{t} \to$ dilepton sample [92], and a sample of jets including muons [93]; nevertheless, as default assumption, we used

$\rho_{\mathrm{ATL}} = \rho_{\mathrm{CMS}} = 1$ in the present results. As opposed to what was done in Ref. [7], the present combination is carried out with $\rho_{\mathrm{LHC}} = 0$ for this source. Variations of this assumption are analysed in the stability checks (see Section 7 for further details). Finally $\rho_{\mathrm{COL}} = 0$ is used for the default result. Despite the sizable reduction of the bJES related systematics that is achieved, the ATLAS $t\bar{t} \to$ lepton+jets analysis exhibits an increased sensitivity to the uncertainties of the b-tagging efficiency and of the light jet rejection factors. This is related to the shape differences introduced by the b-tagging SF variations in the variable sensitive to the bJSF [14].

LepPt: This category takes into account the uncertainties in the efficiency of the trigger, in the identification and reconstruction of electrons and muons, and residual uncertainties due to a possible miscalibration of the lepton energy and momentum scales [39,96–98]. The correlation assumptions for this uncertainty source are $\rho_{\mathrm{EXP}} = 1$, and $\rho_{\mathrm{TEV}} = \rho_{\mathrm{LHC}} = \rho_{\mathrm{COL}} = 0$.

BGMC: (Background from MC) This represents the uncertainty due to the modelling of the background processes determined from MC. This uncertainty source is assumed to be fully correlated between all input measurements in the same $t\bar{t}$ decay channel ($\rho_{\mathrm{EXP}} = \rho_{\mathrm{TEV}} = \rho_{\mathrm{LHC}} = \rho_{\mathrm{COL}} = 1$ in the same analysis channel).

BGData: (Background from data) This class includes the uncertainties of the modelling of the background determined from data, and is assumed to be uncorrelated between all input measurements ($\rho_{\mathrm{EXP}} = \rho_{\mathrm{TEV}} = \rho_{\mathrm{LHC}} = \rho_{\mathrm{LHC}} = 0$). These typically originate from uncertainties in the normalisation of the QCD multijet and Drell-Yan backgrounds determined from data.

Meth: (Method) This systematic uncertainty relates to the m_{top} extraction technique adopted by the analyses (uncorrelated between all measurements: $\rho_{\mathrm{EXP}} = \rho_{\mathrm{TEV}} = \rho_{\mathrm{LHC}} = \rho_{\mathrm{COL}} = 0$). This includes uncertainties caused by the limited MC statistics available for the measurement calibration.

MHI: (Multiple Hadronic Interactions) This systematic uncertainty arises from the modelling of the pile-up conditions in the simulation with respect to the data (overlay of multiple proton-(anti)proton interactions). It is assumed to be fully correlated between all measurements in the same experiments ($\rho_{\mathrm{EXP}} = 1$). Between the Tevatron experiments this uncertainty is treated as uncorrelated due to the different methods of determination ($\rho_{\mathrm{TEV}} = 0$)[6]. For LHC experiments, this uncertainty is MC driven and assumed to be fully correlated ($\rho_{\mathrm{LHC}} = 1$). Finally, for this category $\rho_{\mathrm{COL}} = 0$ is used in the combination.

[6] D0 models the pile-up contribution overlaying real minimum-bias data events in the MC simulation.

6 World m_{top} combination

Using the BLUE method, and the information described above, the combined value of m_{top} is:

$$m_{\text{top}} = 173.34 \pm 0.27\ (\text{stat}) \pm 0.71\ (\text{syst})\ \ \text{GeV}.$$

Alternatively, separating the iJES statistical contribution from the quoted systematic uncertainty, the result reads:

$$m_{\text{top}} = 173.34 \pm 0.27\ (\text{stat}) \pm 0.24\ (\text{iJES}) \pm 0.67\ (\text{syst})\ \ \text{GeV}.$$

The χ^2 of the combination is 4.3 for 10 degrees of freedom (ndf) and the corresponding probability is 93% [21, 22]. This value, calculated taking correlations into account, can be used to assess the extent to which the individual measurements are consistent with the combined m_{top} value and with the hypothesis that they measure the same physics parameter. Moreover, for each input value m_i (with an overall uncertainty σ_i), the pull, calculated as $\text{pull}_i = (m_i - m_{\text{top}})/\sqrt{\sigma_i^2 - \sigma_{m_{\text{top}}}^2}$, where $\sigma_{m_{\text{top}}}$ is the total uncertainty of the combined m_{top} result, indicates the degree of agreement among the input measurements.

Table 3 and Figure 1 summarise the inputs and the results of the combination. In Figure 1(a), this m_{top} combination result, the individual Tevatron and LHC combinations [6,7] and the input measurements are compared. The total uncertainty, the statistical and the iJES contributions (when applicable), as well as the sum of the remaining uncertainties are reported separately. The central value of the world m_{top} combination falls outside the range defined by the central values of the individual Tevatron and LHC combinations from Refs. [6, 7]. This is a consequence of the reduced set of input measurements used in this combination with respect to Ref. [6] (see below for further details). It may be worth noting that the statistical uncertainty (including in quadrature the iJES component) of the world m_{top} combination is slightly larger than the corresponding uncertainty reported in the previous LHC combination [7]. A similar consideration holds for the statistical uncertainty of the input measurements relative to that of the combined result. This can happen due to the combination method, which minimises the total uncertainty of the combined result, not the separate statistical and systematic contributions (see Section 2). In this framework, the breakdown of uncertainties for the combined result, is a function not only of the uncertainties of the input measurements, but also of the correlations among them through the combination [22]. The BLUE combination coefficients used in the linear combination of the input m_{top} values and the pulls are provided in Figures 1(b) and 1(c), respectively. Within the BLUE method, negative coefficients can occur when individual measurements have different precisions and large correlations [21, 99, 100].

The correlations among input m_{top} measurements are reported in Table 5. The precision of the combined result relative to the most precise single measurement is improved by about 28%. The total uncertainty on m_{top} is 0.76 GeV, and corresponds to a relative uncertainty of 0.44%. The resulting total uncertainty is dominated by systematic contributions related to the modelling of the $t\bar{t}$ signal and the knowledge of the jet energy scale for light- and b-quark originated jets (Table 3).

Complementing the information encoded in the BLUE combination coefficients, the impact of the various input measurements is estimated using the Fisher information concept, $I = 1/\sigma_{m_{\text{top}}}^2$ [99]. For each of the input measurements, intrinsic (IIW_i) and marginal information weights (MIW_i) are derived. The intrinsic information weight carried by the i^{th}-measurement is supplemented by the introduction of a weight inherent to the ensemble of all correlations between the input measurements (IIW_{corr}):

$$\text{IIW}_i = \frac{1/\sigma_i^2}{1/\sigma_{m_{\text{top}}}^2} = \frac{1/\sigma_i^2}{I};\ \ \text{IIW}_{\text{corr}} = \frac{I - \sum_i 1/\sigma_i^2}{I}.$$

The IIW_i for each individual measurement is defined as the ratio of the information it carries when taken alone ($1/\sigma_i^2$) to the total information of the combination. While the IIW_i are defined to be positive, IIW_{corr} can be negative, or positive, depending on whether the net effect of the correlations is to increase, or decrease, the total uncertainty of the combination. The marginal information weight, defined as

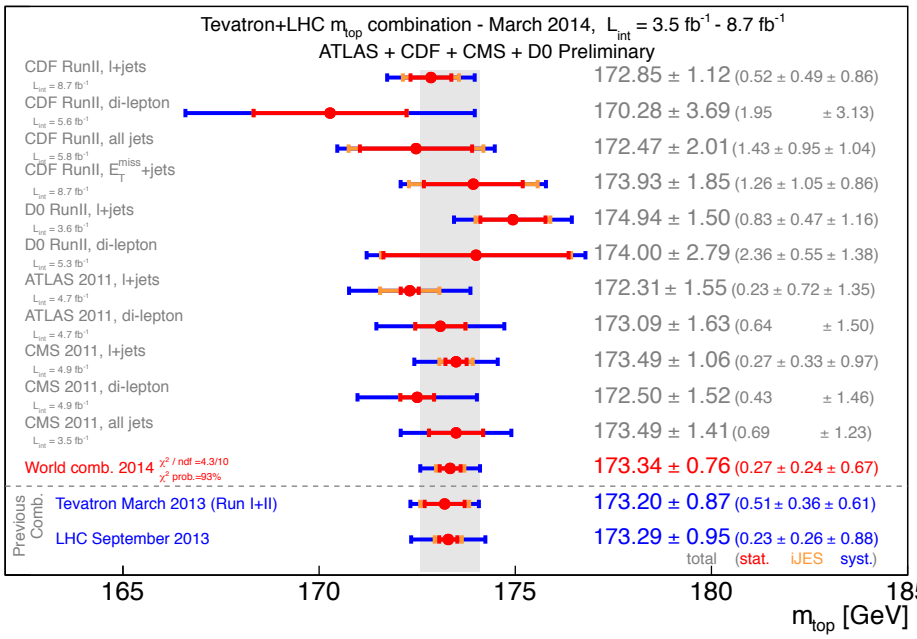

(a)

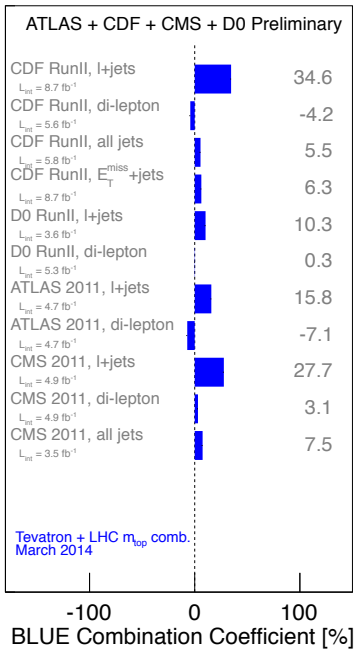

(b)

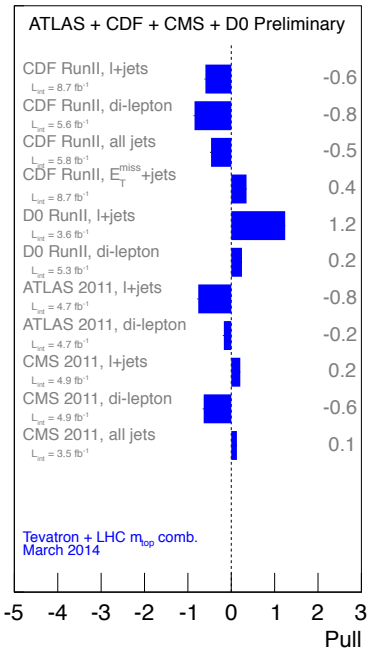

(c)

Figure 1: (a): Input measurements and result of their combination (see also Table 3), compared with the Tevatron and LHC combined $m_{\rm top}$ values [6, 7]. With respect to Ref. [6] only a partial set of Tevatron $m_{\rm top}$ measurements is used in the world combination (see Section 4). For each measurement, the total uncertainty, the statistical and the iJES contributions (when applicable), as well as the sum of the remaining uncertainties are reported separately. The iJES contribution is statistical in nature and applies only to analyses performing in situ ($t\bar{t}$) jet energy calibration procedures. The grey vertical band reflect the total uncertainty on the combined $m_{\rm top}$ value. Panels (b) and (c) show, respectively, the BLUE combination coefficients and pulls of the input measurements.

		CDF				D0		ATLAS		CMS		
		l+jets	di-l	all jets	$E_{\mathrm{T}}^{\mathrm{miss}}$	l+jets	di-l	l+jets	di-l	l+jets	di-l	all jets
CDF	l+jets	1.00										
	di-l	0.49	1.00									
	all jets	0.28	0.25	1.00								
	$E_{\mathrm{T}}^{\mathrm{miss}}$	0.31	0.27	0.17	1.00							
D0	l+jets	0.29	0.09	0.16	0.18	1.00						
	di-l	0.15	0.07	0.10	0.11	0.38	1.00					
ATLAS	l+jets	0.17	0.07	0.10	0.12	0.17	0.11	1.00				
	di-l	0.30	0.12	0.17	0.19	0.24	0.15	0.64	1.00			
CMS	l+jets	0.23	0.12	0.15	0.16	0.21	0.16	0.24	0.34	1.00		
	di-l	0.09	0.05	0.05	0.08	0.08	0.07	0.16	0.24	0.64	1.00	
	all jets	0.15	0.06	0.09	0.10	0.13	0.08	0.15	0.23	0.57	0.75	1.00

Table 5: Correlations among the eleven input measurements. The elements in the table are labelled according to the experiment and the $t\bar{t}$ final state.

Measurements		BLUE comb. coeff. [%]	IIW [%]	MIW [%]
CDF	l+jets	34.6	46.6	16.1
	di-l	−4.2	4.3	3.0
	all jets	5.5	14.4	1.9
	$E_{\mathrm{T}}^{\mathrm{miss}}$	6.3	16.9	2.1
D0	l+jets	10.3	25.8	3.2
	di-l	0.3	7.5	0.0
ATLAS	l+jets	15.8	24.2	6.1
	di-l	−7.1	21.9	1.2
CMS	l+jets	27.7	51.3	7.6
	di-l	3.1	25.1	0.1
	all jets	7.5	29.2	0.8
Correlations ($\mathrm{IIW_{corr}}$)		—	−167.3	—

Table 6: Evaluation of the impact of the individual measurements on the combined m_{top}. The values of the BLUE combination coefficients, the intrinsic information weights IIW_i, and the marginal information weights MIW_i are given. The intrinsic information weight $\mathrm{IIW_{corr}}$ of correlations is also shown on a separate row [99].

$$\mathrm{MIW}_i = \frac{I_{\,n \text{ meas}} - I_{n-1 \text{ meas.: all but } i}}{I_{n \text{ meas}}}$$

can also be used to quantify the information that an individual measurement brings in a combination. MIW_i quantifies the additional information brought by the i^{th}-measurement when added to a combination that includes the other $n-1$ inputs.

The intrinsic and marginal information weights, for each individual input measurement, and the intrinsic information weight of the correlations, are listed in Table 6. For comparison, the corresponding BLUE combination coefficients are also reported. The intrinsic information weight carried by the ensemble of the correlations among measurements, $\mathrm{IIW_{corr}}$, is large in comparison to the contribution of the individual m_{top} inputs (IIW_i). It is therefore important to monitor the stability of the result under variations of the correlation assumptions (see Section 7). While the exact ranking of the input m_{top} measurements varies depending on the figure of merit adopted (BLUE combination coefficient, IIW_i, or MIW_i), Table 6 shows that the current combination result is mainly driven by the m_{top} results in the $t\bar{t} \to$ lepton+jets decay channel.

	Individual	Parameter	Correlations				χ^2/ndf (χ^2 probability)			
	comb. [GeV]	value [GeV]	$m^{l\text{+jets}}$	$m^{\text{di-}l}$	$m^{\text{all jets}}$	$m^{E_{\text{T}}^{\text{miss}}}$	$m^{l\text{+jets}}$	$m^{\text{di-}l}$	$m^{\text{all jets}}$	$m^{E_{\text{T}}^{\text{miss}}}$
$m^{l\text{+jets}}$	173.29 ± 0.80	173.23 ± 0.78	1.00				–			
$m^{\text{di-}l}$	172.74 ± 1.15	172.73 ± 1.09	0.71	1.00			0.43/1 (0.51)	–		
$m^{\text{all jets}}$	173.17 ± 1.20	173.35 ± 1.13	0.58	0.66	1.00		0.02/1 (0.90)	0.46/1 (0.50)	–	
$m^{E_{\text{T}}^{\text{miss}}}$	173.93 ± 1.85	174.03 ± 1.80	0.29	0.26	0.22	1.00	0.21/1 (0.65)	0.49/1 (0.48)	0.13/1 (0.72)	–

Table 7: Individual and correlated combination results according to the various $t\bar{t}$ final states. The correlated determination of the m_{top} per decay channel (parameter value) is reported together with the pair-wise correlation coefficients, and the compatibility tests in terms of χ^2/ndf and its associated probability. For comparison, the results of the separate combinations (individual comb.) of the individual inputs from Table 3 are reported in the second column.

	Individual	Parameter	Correlations				χ^2/ndf (χ^2 probability)			
	comb. [GeV]	value [GeV]	m^{CDF}	m^{D0}	m^{ATL}	m^{CMS}	m^{CDF}	m^{D0}	m^{ATL}	m^{CMS}
m^{CDF}	173.19 ± 1.00	172.96 ± 0.98	1.00				–			
m^{D0}	174.85 ± 1.48	174.62 ± 1.46	0.31	1.00			1.25/1 (0.27)	–		
m^{ATL}	172.65 ± 1.44	172.70 ± 1.43	0.29	0.23	1.00		0.03/1 (0.86)	1.14/1 (0.29)	–	
m^{CMS}	173.58 ± 1.03	173.54 ± 1.02	0.25	0.22	0.32	1.00	0.23/1 (0.64)	0.46/1 (0.50)	0.32/1 (0.57)	–

Table 8: Individual and correlated combination results according to the various experiments. The correlated determination of the m_{top} per experiment (parameter value) is reported together with the pair-wise correlation coefficients, and the compatibility tests in terms of χ^2/ndf and its associated probability. For comparison, the results of the separate combinations (individual comb.) of the individual inputs from Table 3 are reported in the second column.

	Individual	Parameter	Correlations		χ^2/ndf (χ^2 probability)	
	comb. [GeV]	value [GeV]	m^{TEV}	m^{LHC}	m^{TEV}	m^{LHC}
m^{TEV}	173.58 ± 0.94	173.41 ± 0.91	1.00		–	
m^{LHC}	173.28 ± 0.94	173.26 ± 0.94	0.36	1.00	0.02/1 (0.89)	–

Table 9: Individual and correlated combination results according to the Tevatron and LHC colliders. The correlated determination of the m_{top} per collider (parameter value) is reported together with the pair-wise correlation coefficients, and the compatibility tests in terms of χ^2/ndf and its associated probability. For comparison, the results of the separate combinations (individual comb.) of the individual inputs from Table 3 are reported in the second column. See text for further details.

Using the same inputs, uncertainty categorisation, and correlation assumptions, additional combinations have been performed as detailed below.

- **Individual combinations** by $t\bar{t}$ final state, experiment, and collider, have been derived neglecting other input measurements. These results can be used to quantify the improvement obtained by the overall combination with respect to the results obtained using only a partial set of the input measurements.

- **Correlated combinations** are obtained within the BLUE program by simultaneously extracting different mass parameters instead of a common m_{top}. The m_{top} parameter values obtained using this procedure (per $t\bar{t}$ final state, experiment, or collider), are affected by the full set of input measurements through their correlations, and can be used to test the consistency between the various m_{top} determination. In the following this is done using a pair-wise χ^2 formulation and its associated probability: $\chi^2(m_1, m_2) = (m_1 - m_2)^2/\sigma_{12}^2$, where $\sigma_{12}^2 = \sigma_1^2 + \sigma_2^2 - 2\rho_{12}\sigma_1\sigma_2$, and ρ_{12} is the correlation between the two measurements.

The results are summarised in Tables 7, 8 and 9, respectively, for the combination according to the $t\bar{t}$ final state ($m^{l\text{+jets}}$, $m^{\text{di-}l}$, $m^{\text{all jets}}$, $m^{E_{\text{T}}^{\text{miss}}}$), to the individual experiments (m^{CDF}, m^{D0}, m^{ATL}, m^{CMS}), and to the

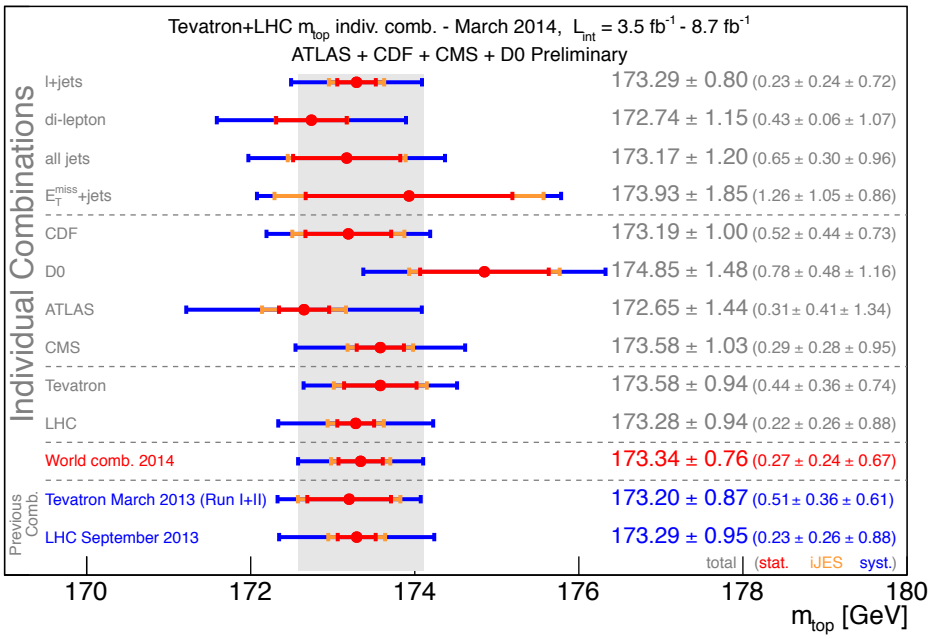

Figure 2: Comparison of the world m_{top} combination result with the individual m_{top} determinations per $t\bar{t}$ decay channel, experiment, and collider. Results are compared with the Tevatron and LHC combined m_{top} values from Refs. [6, 7]. The grey vertical band reflect the total uncertainty on the combined m_{top} value.

Tevatron and LHC colliders (m^{TEV}, m^{LHC}). Figure 2 reports the comparison of the world m_{top} combination with the individual m_{top} determinations per $t\bar{t}$ decay channel, experiment, and collider. In addition m_{top} combination results from Refs. [6, 7] are also reported (see Appendix B, Figure 4 for the correlated m_{top} determinations). The full uncertainty breakdown of the individual CDF, D0, ATLAS, CMS, Tevatron and LHC combinations is reported in Appendix C. The individual combination for m^{TEV} and m^{LHC} present some differences with respect to the results documented in Refs. [6, 7]. For m^{TEV}, these mainly originate from the reduced set of input measurements used in the combination with respect to Ref. [6], and to a lesser extent from the use of a finer MC modelling uncertainty splitting (four separate categories: MC, Rad, CR, PDF, rather than a single one including all of them), and the change in the JES uncertainty categories for the CDF measurements. The slight differences in the uncertainty breakdown of the separate combination of m^{LHC} with respect to Ref. [7] are mainly attributed to the changes of the uncertainty categorisation and correlation assumption underlying the stdJES and b-tagging categories.

7 Effects of using alternative correlation models and uncertainty treatments

The categorisation and the correlation assumptions summarised in Tables 3 and 4 reflect the present understanding and the limitations due to the different choices made by the experiments when evaluating the individual uncertainty sources. In this preliminary result, the effects of the approximations are evaluated by performing stability cross checks, in which the input assumptions are changed with respect to the values reported in Section 5. The results of these cross checks are described in the following, and summarised in Figure 3.

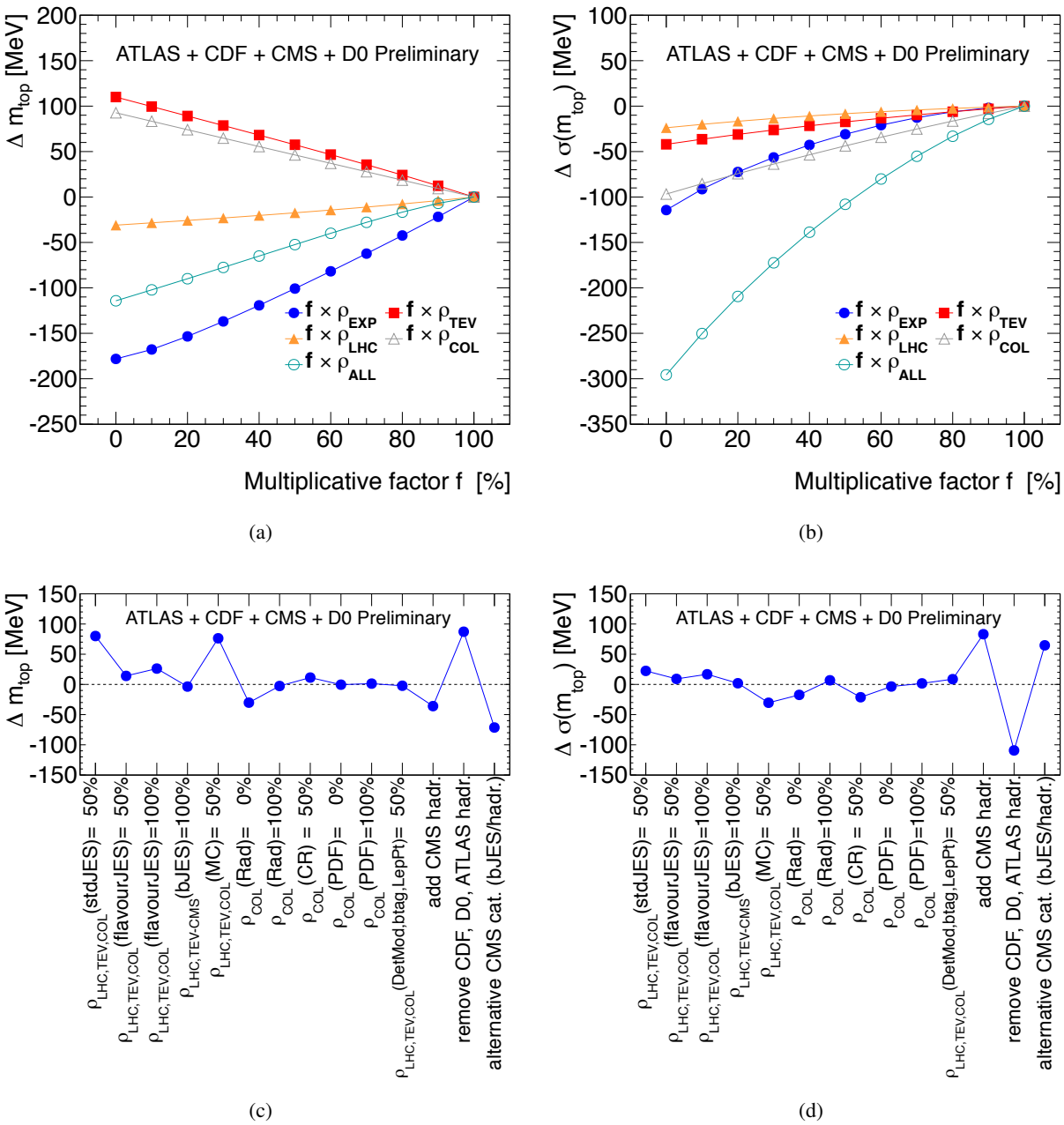

Figure 3: Variation of the combined m_{top} result (a,c) and its total uncertainty (b,d) as a function of variations in the correlation assumptions. (a,b) ρ_{EXP}, ρ_{LHC}, ρ_{TEV} and ρ_{COL} are varied simultaneously using a multiplicative factor f in the range [0,1] (open light blue dots). Separate variations of each correlation coefficient in the same range, are reported by the blue (filled dots), orange (filled triangles), red (filled squares) and the grey (open triangles) curve, respectively. (c,d) Stability of the world combination under variations of the default assumptions on the correlation for selected uncertainty sources. The sensitivity of the combination to different scenarios concerning the treatment of the hadronisation systematics is also shown. See text for details.

7.1 Overall correlations

The stability of the combined $m_{\rm top}$ result with respect to the correlation assumptions reported in Table 4 has been checked by changing, simultaneously for all systematic sources, the values of $\rho_{\rm EXP}$, $\rho_{\rm LHC}$, $\rho_{\rm TEV}$ and $\rho_{\rm COL}$ by a multiplicative factor, f, in the range [0, 1] (referred to as $\rho_{\rm ALL}$ in the following Figures). The result of this stability check in terms of the shifts of the combined $m_{\rm top}$ value ($\Delta m_{\rm top}$) and of its total uncertainty ($\Delta\sigma_{m_{\rm top}}$) are reported in Figure 3(a,b). While the correlated variation of all assumptions is somewhat arbitrary, it allows the inspection of the extreme case of a combination of totally uncorrelated measurements ($f = 0$): the result is $\Delta m_{\rm top} = -114$ MeV and $\Delta\sigma_{m_{\rm top}} = -296$ MeV.

The sensitivity of the combination to the assumed correlations between measurements from the same experiment, across experiments, and across colliders, has been evaluated using separate variations of $\rho_{\rm EXP}$, $\rho_{\rm LHC}$, $\rho_{\rm TEV}$ and $\rho_{\rm COL}$, respectively. The separate correlation variations as a function of the value of the multiplicative factor f are reported by the blue, orange, red and the grey curve in Figure 3(a,b), respectively. The largest effects on $\Delta\sigma_{m_{\rm top}}$ are related to the separate variation of $\rho_{\rm EXP}$ and $\rho_{\rm COL}$, for which, $f = 0$ results in $\Delta m_{\rm top} = -178$ MeV, $\Delta\sigma_{m_{\rm top}} = -114$ MeV and $\Delta m_{\rm top} = +93$ MeV, $\Delta\sigma_{m_{\rm top}} = -97$ MeV, respectively, signalling a larger sensitivity of the result to the intra-experiment and intra-collider correlations.

An alternative study, varying separately the $\rho_{\rm EXP}$, $\rho_{\rm LHC}$, $\rho_{\rm TEV}$ and $\rho_{\rm COL}$ correlations for individual uncertainty sources is reported in Appendix D.

7.2 JES component correlations

The methodologies and assumptions used to derive the jet energy corrections and the related uncertainties are not always directly comparable between experiments. As a consequence, variations of the corresponding $\rho_{\rm LHC}$, $\rho_{\rm TEV}$ and $\rho_{\rm COL}$ assumptions, have been considered in the combination stability checks. These affected the stdJES ($\rho = 0 \to 0.5$), and the flavourJES components of the JES (from $\rho = 0$ to $\rho = 0.5$ or $\rho = 1$). The maximum deviations observed with respect to the default result are: $\Delta m_{\rm top} = +80$ MeV and $\Delta\sigma_{m_{\rm top}} = +22$ MeV.

A different strategy is also followed concerning the evaluation of the b-jet specific energy scale uncertainty. Within the Tevatron experiments and ATLAS, the effects stemming from b-quark fragmentation, hadronisation and underlying soft radiation (the latter for ATLAS only) are studied using different MC event generation models [65]. On the other hand, in CMS, the Pythia and Herwig fragmentation models are used to evaluate the response variation for different jet flavor mixtures. The largest differences are found for pure quark and gluon flavours. The maximum of these differences, for pure quark flavour at low $p_{\rm T}$ and for pure gluon flavour at high $p_{\rm T}$, is taken as a flavor uncertainty applicable to any jet flavor or flavor mixture [34]. To reflect these differences in the estimate of the b-JES uncertainty, $\rho_{\rm LHC} = \rho_{\rm CMS-TEV} = 0.5$ is used as the default assumption for this source of systematic uncertainty. The changes of the combination when using $\rho_{\rm LHC} = \rho_{\rm CMS-TEV} = 1.0$ are studied as another stability test. The results of this are $\Delta m_{\rm top} = -4$ MeV, $\Delta\sigma_{m_{\rm top}} = +2$ MeV.

7.3 Signal modelling

7.3.1 Experimental and collider correlations

For the evaluation of the MC systematic uncertainty, different MC generators are used within the various collaborations (Section 3 and Table 1). In addition a contribution to the uncertainty due to the choice of the hadronisation model used in the simulation is included for the Tevatron and the ATLAS input measurements. Finally, different input PDF (CTEQ5L and CTEQ6L1 for CDF and D0, and CT10 and CTEQ6.6L for ATLAS and CMS, respectively) are used in the baseline MC by the various collaborations. These aspects may reduce the actual correlation between input measurements for these uncertainty classes. As a result, the combination has been repeated using $\rho_{\rm LHC} = \rho_{\rm TEV} = \rho_{\rm COL} = 0.5$ for the MC and CR uncertainty sources: the maximum observed deviations with respect to the default result are $\Delta m_{\rm top} = +76$ MeV, and $\Delta\sigma_{m_{\rm top}} = -30$ MeV and correspond to the variation of the correlation for the signal MC uncertainty. In addition, variation of $\rho_{\rm COL}$ (from

0.5 to 0 or 1.0) for the systematic uncertainties associated to the choice of the proton (anti-proton) PDF and the modelling of the QCD radiation effects have been considered. The results of this test are $|\Delta m_{\rm top}| \leq +30$ MeV, $|\Delta\sigma_{m_{\rm top}}| \leq +17$ MeV.

7.3.2 Hadronisation and alternative uncertainty categorisation

As mentioned above, in the signal modelling categorisation, additional uncertainties can arise from the choice of the hadronisation model (cluster or string fragmentation as implemented in Herwig and Pythia, respectively) describing the transition from final state partons to colourless hadrons. The change in $m_{\rm top}$ obtained by exchanging cluster and string models in a fixed MC setup can be quoted as a hadronisation uncertainty for the $m_{\rm top}$ measurements. However, this source of uncertainty is typically also considered among the components of the jet energy scale uncertainty (both for inclusive- and b-quark jets) and sizable double counting effects may result. For the time being, the experiments choose different approaches. Tevatron experiments and ATLAS quote an explicit hadronisation systematic related to the $t\bar{t}$ modelling in the MC. Within CMS, to minimise double counting, no additional hadronisation systematic is quoted. Given the relatively large size of this uncertainty (ranging between 0.27 and 0.58 GeV depending on the analysis), a harmonisation of the treatment of this systematics is needed in the future. Specifically, an in-depth investigation of the level of the double counting effects involved when both types of components are used is important for the next generation of measurements and $m_{\rm top}$ combinations. These studies are currently in progress. To estimate the possible significance of these effects, the $m_{\rm top}$ combination has been repeated for several different assumptions. From the comparison of Powheg simulations with Pythia and Herwig used for the fragmentation stage, CMS has derived estimates of the hadronisation uncertainty of 0.58, 0.76 and 0.93 GeV for the l+jets, di-l, and all jets channels, respectively [7]. Adding these into the corresponding MC systematic uncertainty, and repeating the combination results in $\Delta m_{\rm top} = -36$ MeV and $\Delta\sigma_{m_{\rm top}} = +83$ MeV. The relatively large effect is introduced by an increased total uncertainty for the CMS input measurements, and the consequent change of the BLUE combination coefficients of the input measurements. In this case and for the eleven input measurements, yielding: 41.5%, -4.7%, 7.0%, 8.2% for the CDF l+jets, di-l, all jets, and $E_{\rm T}^{\rm miss}$ measurements; 12.7%, 0.9%, 20.1%, -5.5%, for the D0 and ATLAS l+jets and di-l measurements; and finally 22.5%, 1.5%, and 4.1% for the CMS l+jets, di-l, and all jets measurements respectively[7].

On the other hand, if the extra hadronisation systematics evaluated by CDF, D0, and ATLAS in addition to the JES components, are removed, the observed changes are $\Delta m_{\rm top} = +87$ MeV and $\Delta\sigma_{m_{\rm top}} = -109$ MeV.

In addition to the above investigations, CMS has studied an alternative systematic categorisation. While keeping the hadronisation uncertainties described above, the bJES uncertainty is evaluated at the analysis level using the uncertainties in the b-fragmentation function, and the b-semileptonic branching fractions. The uncertainty in the b-fragmentation is evaluated by varying the Bowler-Lund parameters used to model the b-quark fragmentation in Pythia between the Pythia Z2 tune and the results of the Perugia2011 [42] and Corcella [66] tunes. This results in an uncertainty of $m_{\rm top}$ of 0.15 GeV. An additional uncertainty of 0.10 GeV comes from varying the b-semileptonic branching fractions within their measured uncertainties. In this framework, the combined uncertainty of 0.18 GeV is taken as the bJES uncertainty for all CMS input measurements. The impact of changing to this characterisation of the hadronisation and bJES uncertainties for the CMS analyses is found to be $\Delta m_{\rm top} = -71$ MeV and $\Delta\sigma_{m_{\rm top}} = +65$ MeV. Further work is needed to resolve this issue and detailed studies are ongoing.

Due to the sensitivity of the combined result to the treatment of hadronisation uncertainties, progress on these aspects will be of key importance for future analyses of increased precision, and for $m_{\rm top}$ combination updates.

[7] For the eleven input measurements the corresponding values, in %, of the intrinsic information weights are: 57.3, 5.3, 17.7, 20.8 for CDF, 31.8, 9.2 for D0, 29.8 27.0 for ATLAS, 48.7, 24.7, and 25.0 for CMS. The corresponding $\mathrm{IIW_{corr}}$ is -197.2.

7.4 Detector modelling correlations

The detector modelling, lepton related and b-tagging based systematics could include some level of correlation between experiments introduced by the use of MC simulation in the evaluation of the detector performance. For this reason, a test is performed increasing the default correlations for these three uncertainty sources ($\rho_{\rm TEV}$, $\rho_{\rm LHC}$, $\rho_{\rm COL}$) from 0% to 50%. The effect of this change is found to be $\Delta m_{\rm top} = -2$ MeV and $\Delta\sigma_{m_{\rm top}} = +9$ MeV.

7.5 Minimisation of the Fisher information

As an additional cross check, the stability of the combination has been verified applying the recipes described in Ref. [99]. Numerical minimisation procedures aimed at reducing the Fisher information (recall $I = 1/\sigma^2_{m_{\rm top}}$) of the combination are applied varying the correlation assumptions by multiplicative factors in three different scenarios. In the simplest case, all correlations are rescaled by the same global factor (minimise by global factor). As a second option, the same rescaling factor is applied to all correlations within each error source (minimise by error source). Finally, an alternative minimisation procedure is performed in which for all error sources the off-diagonal correlations ($\rho_{ij},\ i \neq j$) are rescaled by the same factor (minimise by off-diagonal element). The maximum deviations with respect to default results are obtained for the third scenario, and correspond to $\Delta m_{\rm top} = -60$ MeV and $\Delta\sigma_{m_{\rm top}} = +20$ MeV.

Alternative cross checks, as proposed in Ref. [99] and adopted in Ref. [101], have been performed and yield consistent results with respect to the default combination.

7.6 Concluding remarks on combination stability checks

As described in the previous sub-sections, several tests varying simultaneously the correlation assumptions for all systematic uncertainties have been performed, changing $\rho_{\rm ALL}$, as well as just $\rho_{\rm EXP}$, $\rho_{\rm TEV}$, $\rho_{\rm LHC}$ or $\rho_{\rm COL}$. While setting $\rho_{\rm ALL} = 0$ ($f = 0$) allows the inspection of the ideal case of a combination of totally uncorrelated measurements, the simultaneous reduction of the correlations by a factor of $1/2$ or $4/5$ ($f = 50\%$, or 80%), induces changes of the central $m_{\rm top}$ value and of its total uncertainty at the level of ± 100 MeV or ± 40 MeV, respectively (see Figures 3(a) and 3(b)). The effect of the separate variation of the correlations for individual uncertainty sources has been studied (Appendix D), and found to be consistent (and reduced) relative to the above results. The stability of the world $m_{\rm top}$ combination under variations of the default correlation assumptions for selected uncertainty sources has also been studied. The largest effects are related to changes of the correlation assumptions for the dominant uncertainty sources: the stdJES ($\rho_{\rm TEV}$, $\rho_{\rm LHC}$, $\rho_{\rm COL} = 0 \rightarrow 0.5$), and the MC systematic uncertainties ($\rho_{\rm TEV}$, $\rho_{\rm LHC}$, $\rho_{\rm COL} = 1 \rightarrow 0.5$). These result in $\Delta m_{\rm top} = +80$ MeV, $\Delta\sigma_{m_{\rm top}} = +22$ MeV and $\Delta m_{\rm top} = +76$ MeV, $\Delta\sigma_{m_{\rm top}} = -30$ MeV, respectively (see Figures 3(c) and 3(d)). In addition, the sensitivity of the combined result to the different treatments of hadronisation uncertainties across experiments, has been studied and estimated at the level of ± 100 MeV for both $\Delta m_{\rm top}$ and $\Delta\sigma_{m_{\rm top}}$. The effect is connected to sizable changes of the BLUE combination coefficients of the input measurements.

Due to the relatively small size of the effects relative to the current $m_{\rm top}$ precision, no additional systematic uncertainty is associated to the final combined result. Discussions of the methodologies used to evaluate systematic uncertainties and the possibility to determine directly the correlations among individual measurements are ongoing. These are aimed at an improved treatment of the systematic uncertainties across the experiments, and of their combination.

8 Conclusions

A world combination of the top-quark mass measurements from the Tevatron and the LHC experiments has been presented. The result includes six measurements from Tevatron Run II and five from the 2011 run of the LHC.

The resulting combination, taking account of statistical and systematic uncertainties and their correlations, yields:

$$m_{\text{top}} = 173.34 \pm 0.27\ (\text{stat}) \pm 0.71\ (\text{syst})\ \ \text{GeV},$$

or, separating out the iJES statistical contribution from the quoted systematic uncertainty:

$$m_{\text{top}} = 173.34 \pm 0.27\ (\text{stat}) \pm 0.24\ (\text{iJES}) \pm 0.67\ (\text{syst})\ \ \text{GeV}.$$

The world combination achieves an improvement of the total m_{top} uncertainty of 28% relative to the most precise single input measurement [16] and $\approx$ 13% relative to the previous most precise combination [6]. The total uncertainty of the combination is 0.76 GeV, and is currently dominated by systematic uncertainties due to jet calibration and modelling of the $t\bar{t}$ events. Given the current experimental uncertainty on m_{top}, clarifying the relation between the top quark mass implemented in the MC and the formal top quark pole mass demands further theoretical investigations. The dependence of the result on the correlation assumptions between measurements from the same experiment and across experiments has been studied and found to be small compared to the current m_{top} precision. At the same time, the results of the stability tests reveal the importance of the ongoing discussions on the methodologies used for the evaluation of the systematic uncertainties. In some cases, experiments adopt different approaches which deserve further studies and harmonisation.

A Uncertainty naming conventions

In this Appendix the naming conventions for each systematic uncertainty are summarised. The convention used for the present analysis is compared with those from Refs. [6, 7, 39] (see Table 10).

WA	LHC comb [7]	TEV comb. [6] ([39])	
Stat	Statistics	Statistics	(Statistical uncertainty)
iJES	iJES	iJES	(*in situ* light-jet calibration)
stdJES	uncorrJES⊕insituγ/ZJES⊕intercalibJES	dJES⊕cJES⊕rJES	(Light-jet response 1⊕2)⊕Out-of-cone correction
flavourJES	flavourJES	aJES	(Response to $b/q/g$ jets)
bJES	bJES	bJES	(Model for b jets)
MC	MC⊕UE	part of Signal	(part of Signal modelling)
Rad	Rad	part of Signal	(part of Signal modelling)
CR	CR	part of Signal	(part of Signal modelling)
PDF	PDF	part of Signal	(part of Signal modelling)
DetMod	DetMod	DetMod	(Jet modelling)
b-tag	b-tagging	part of BGData	(part of background based on data)
LepPt	Lepton reconstruction	LepPt	(Lepton modelling)
BGMC	Background from MC	BGMC	(Background from theory)
BGData	Background from Data	BGData	(Background based on data)
Meth	Method	Method	(Calibration Method)
MHI	Multiple Hadronic Interactions	MHI	(Multiple interaction model)

Table 10: Uncertainty naming conventions used for this combination, and from Refs. [6, 7, 39].

B Additional figures

In this appendix, the result of the standard combination is compared with those from the correlated m_{top} determination per $t\bar{t}$ decay channel, experiments and collider. With respect to Figure 2, the m_{top} parameters are influenced by the full set of input measurements through their correlations.

In addition, Figure 5 reports an alternative summary plot. With respect to Figures 1(a), the comparison with previous individual Tevatron and LHC combinations [6, 7] is removed.

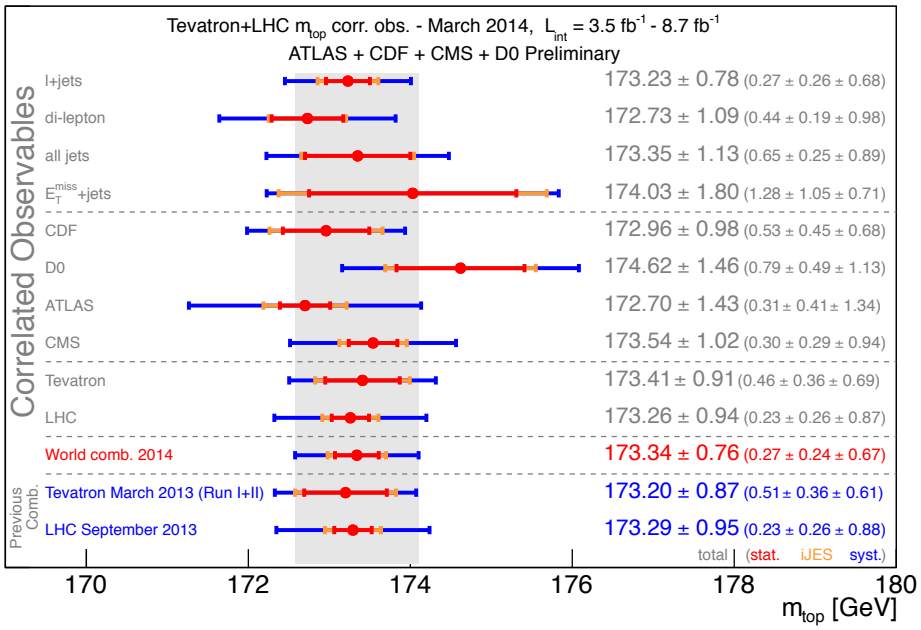

Figure 4: Comparison of the standard combination results with the correlated m_{top} determinations (parameter values in Tables 7, 8 and 9) per $t\bar{t}$ decay channel, experiment, and collider. The grey vertical band reflect the total uncertainty on the combined m_{top} value.

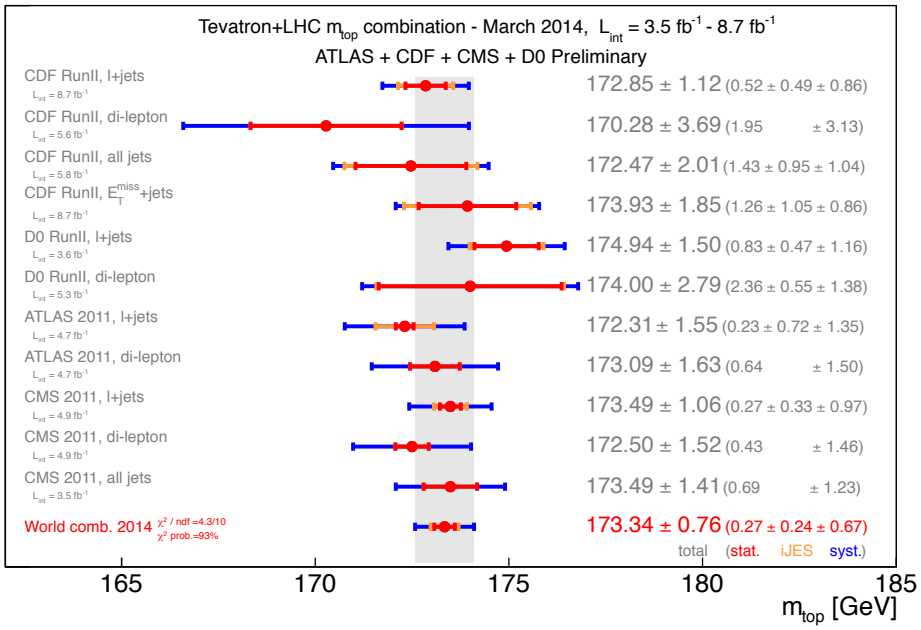

Figure 5: Input measurements and result of the world combination (see also Table 3). For each measurement, the total uncertainty, the statistical and the iJES contributions (when applicable) as well as the sum of the remaining uncertainties are reported separately. The iJES contribution is statistical in nature and applies to analyses performing in situ ($t\bar{t}$) jet energy calibration procedures. The grey vertical band indicates the total world m_{top} uncertainty. With respect to Figures 1(a), the comparison with previous individual Tevatron and LHC combinations [6, 7] is removed.

C Results of the individual experiment combinations

In this Appendix the separate experiment and collider combinations are reported and compared to the $m_{\rm top}$ world results (Table 11). The results of the individual combinations are obtained neglecting other input measurements and their correlations.

All values in GeV	CDF	D0	ATLAS	CMS	Tevatron	LHC	WA
$m_{\rm top}$	173.19	174.85	172.65	173.58	173.58	173.28	173.34
Stat	0.52	0.78	0.31	0.29	0.44	0.22	0.27
iJES	0.44	0.48	0.41	0.28	0.36	0.26	0.24
stdJES	0.30	0.62	0.78	0.33	0.27	0.31	0.20
flavourJES	0.08	0.27	0.21	0.19	0.09	0.16	0.12
bJES	0.15	0.08	0.35	0.57	0.13	0.44	0.25
MC	0.56	0.62	0.48	0.19	0.57	0.25	0.38
Rad	0.09	0.26	0.42	0.28	0.13	0.32	0.21
CR	0.21	0.31	0.31	0.48	0.23	0.43	0.31
PDF	0.09	0.22	0.15	0.07	0.12	0.09	0.09
DetMod	<0.01	0.37	0.22	0.25	0.09	0.20	0.10
b-tag	0.04	0.09	0.66	0.11	0.04	0.22	0.11
LepPt	<0.01	0.20	0.07	<0.01	0.05	0.01	0.02
BGMC	0.10	0.16	0.06	0.11	0.11	0.08	0.10
BGData	0.15	0.19	0.06	0.03	0.12	0.04	0.07
Meth	0.07	0.15	0.08	0.07	0.06	0.06	0.05
MHI	0.08	0.05	0.02	0.06	0.06	0.05	0.04
Total Syst	0.85	1.25	1.40	0.99	0.82	0.92	0.71
Total	1.00	1.48	1.44	1.03	0.94	0.94	0.76
χ^2/ndf	1.09 / 3	0.13 / 1	0.34 / 1	1.15 / 2	2.45 / 5	1.81 / 4	4.33 / 10
χ^2 probability [%]	78	72	56	56	78	77	93

Table 11: Results of the individual experiment and collider combinations using the inputs listed in Table 3. The uncertainty breakdown is provided and compared with the results of the $m_{\rm top}$ world combination.

D Additional stability tests

In this Appendix, the stability tests reported in Section 7.1, are complemented by separately varying the ρ_{EXP}, ρ_{LHC}, ρ_{TEV} and ρ_{COL} correlations for the individual uncertainty sources [100]. This study rests on the assumptions that all uncertainty classes are uncorrelated with respect to each other, and allow the identification of those uncertainty categories for which the correct assessment of the correlation is important for the stability of the result.

In Figures 6 and 7 the variation of the combined m_{top} value (left panels) and of its uncertainty (right panels) are reported for three different variations of the correlation assumptions for each of the uncertainty categories ($f \cdot \rho$, with $f = 0.8,\ 0.5$, and 0). Figure 6 reports the investigations for ρ_{EXP} (top panels), ρ_{LHC} (middle panels), and ρ_{TEV} (bottom panels). Figure 7 displays the results for the variation of ρ_{COL} (top panels), and for the simultaneous variations of all correlation assumptions, ρ_{ALL} (bottom panels).

The largest observed variations of the combined m_{top} result are of the order of about 150 MeV (for $f = 0$), and are related to changes of the correlation assumptions of the JES uncertainty categories (Figure 6(a), for ρ_{EXP}), the MC (Figure 6(c), and Figure 7(a) for ρ_{TEV} and ρ_{COL}, respectively), the Radiation (Figure 6(e), for ρ_{LHC}), and the CR (Figure 7(a), for ρ_{COL}) systematics, respectively. As expected, a combination of the above effects is observed when varying all correlation assumptions between input measurements (ρ_{ALL}), regardless the experiment or collider they originate from (Figure 7(c)).

The variation of the total combined uncertainties are typically more contained ($\Delta(\sigma(m_{\mathrm{top}})) < 100$ MeV), and negative (reducing the correlation increases the precision of the combined result). The sources reporting the largest sensitivities are related to the variation of ρ_{LHC}, ρ_{TEV}, ρ_{COL}, and ρ_{ALL}, for the JES and MC modelling uncertainties (MC, Radiation, CR). An exception is made concerning the stdJES and b-tagging systematic categories, for which the reduction of the correlation assumption can yield a slight increase (of the order of about 5 MeV) of $\Delta(\sigma(m_{\mathrm{top}}))$. This is a consequence of the relatively high correlations between the input measurements [99]. The effect is however negligible relative to the present total uncertainty on m_{top}.

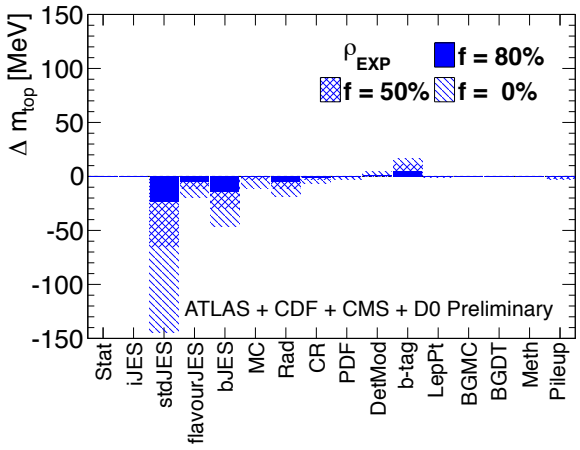

(a) Δm_{top} varying ρ_{EXP}

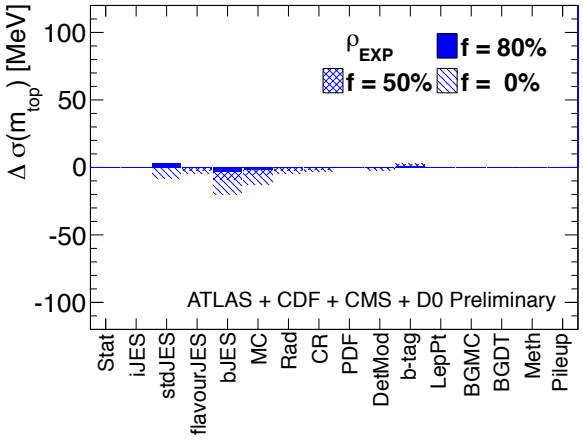

(b) $\Delta\sigma(m_{\text{top}})$ varying ρ_{EXP}

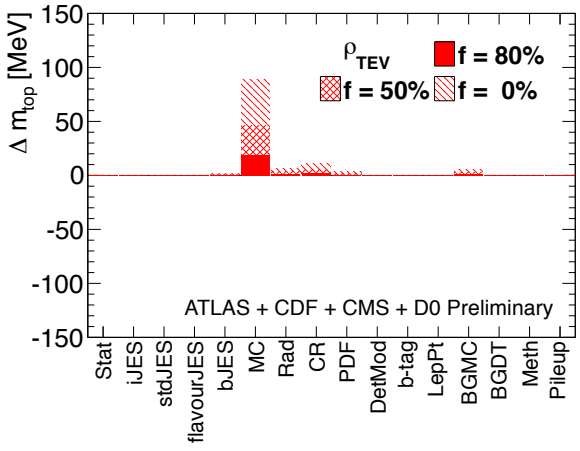

(c) Δm_{top} varying ρ_{TEV}

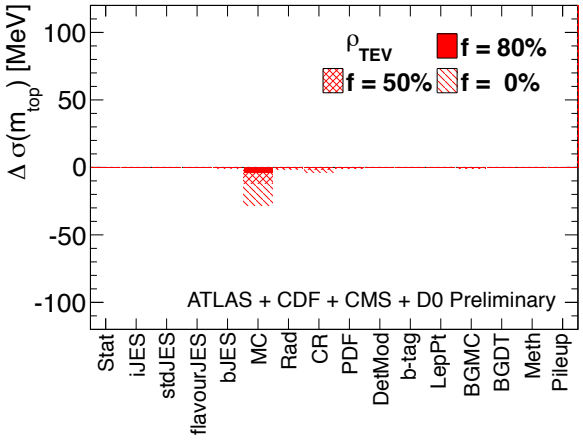

(d) $\Delta\sigma(m_{\text{top}})$ varying ρ_{TEV}

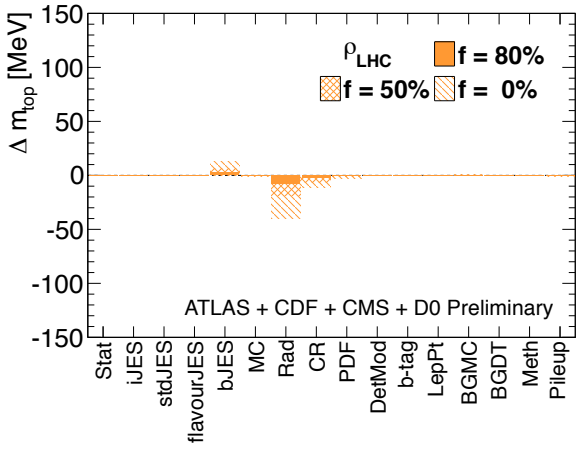

(e) Δm_{top} varying ρ_{LHC}

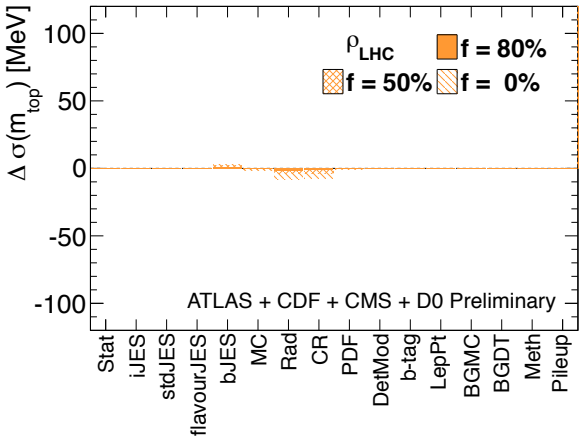

(f) $\Delta\sigma(m_{\text{top}})$ varying ρ_{LHC}

Figure 6: Variation of the combined m_{top} value (a, c, e) and of its uncertainty (b, d, f) for three different correlation assumptions for each uncertainty category ($f \cdot \rho$, with f = 0.8, 0.5, and 0). Variation of ρ_{EXP}, ρ_{TEV} and ρ_{LHC} are reported by the top, middle and bottom panels, respectively.

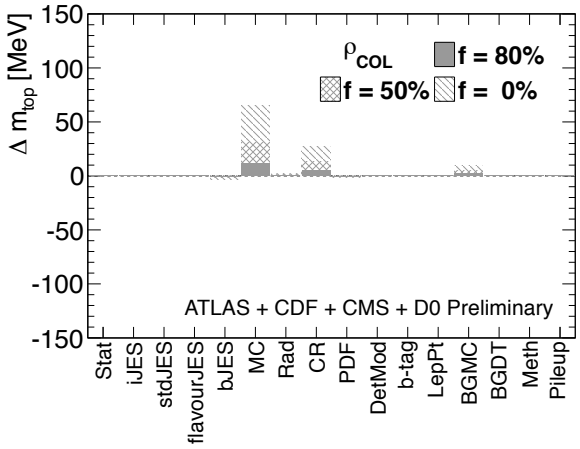

(a) Δm_{top} varying ρ_{COL}

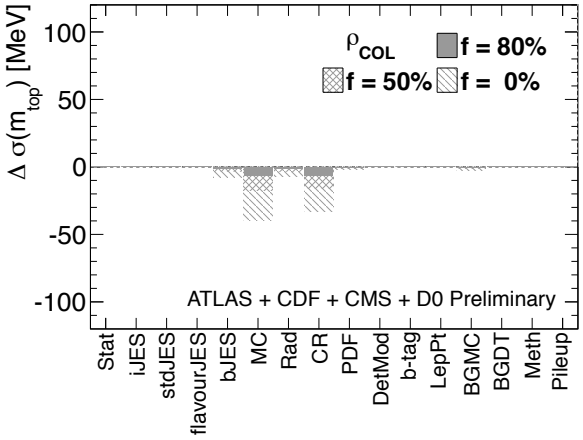

(b) $\Delta\sigma(m_{\text{top}})$ varying ρ_{COL}

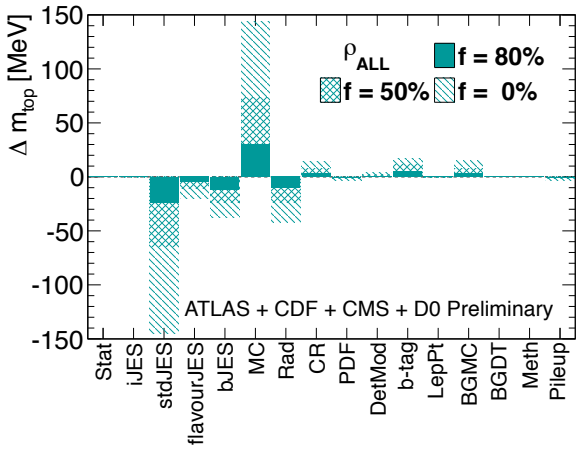

(c) Δm_{top} varying ρ_{ALL}

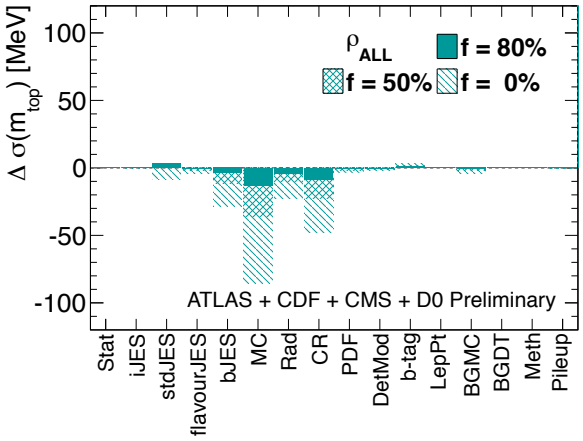

(d) $\Delta\sigma(m_{\text{top}})$ varying ρ_{ALL}

Figure 7: Variation of the combined m_{top} value (a, c) and of its uncertainty (b, d) for three different correlation assumptions for each uncertainty category ($f \cdot \rho$, with $f = 0.8,\ 0.5$, and 0). Variation of ρ_{COL}, and for all correlation between uncertainty sources (ρ_{ALL}) are reported by the top, and bottom panels, respectively.

References

[1] ALEPH, CDF, D0, DELPHI, L3, OPAL, SLD Collaborations, the LEP Electroweak Working Group, the Tevatron Electroweak Working Group and the SLD Electroweak and Heavy Flavour Groups, *Precision electroweak measurements and constraints on the Standard Model*, arXiv:1012.2367 [hep-ex].

[2] M. Baak et al., *The Electroweak Fit of the Standard Model after the Discovery of a New Boson at the LHC*, Eur. Phys. J. **C72** (2012) 2205, arXiv:1209.2716 [hep-ph]. Updates available from http://gfitter.desy.de.

[3] G. Degrassi et al., *Higgs mass and vacuum stability in the Standard Model at NNLO*, JHEP **2012** no. 8, (2012) 1, arXiv:1205.6497 [hep-ex].

[4] F. Bezrukov et al., *The Standard Model Higgs boson as the inflaton*, Phys. Lett. B **659** (2008) 703, arXiv:0710.3755 [hep-th].

[5] A. De Simone et al., *Running Inflation in the Standard Model*, Phys. Lett. B **678** (2009) 1, arXiv:0812.4946 [hep-ph].

[6] Tevatron Electroweak Working Group, *Combination of CDF and D0 results on the mass of the top quark using up to 8.7* fb^{-1} *at the Tevatron*, conference notes CDF Note 10976 and D0 Note 6381, 2013. arXiv:1305.3929 [hep-ex].

[7] ATLAS and CMS Collaborations, *Combination of ATLAS and CMS results on the mass of the top quark using up to 4.9* fb^{-1} *of data*, conference notes CMS-PAS-TOP-13-005 and ATLAS-CONF-2013-102, 2013. https://cds.cern.ch/record/1601811;https://cds.cern.ch/record/1603490.

[8] CDF Collaboration, *Precision Top-Quark Mass Measurements at CDF*, Phys. Rev. Lett. **109** (2012) 152003, arXiv:1207.6758 [hep-ex].

[9] CDF Collaboration, *Top quark mass measurement using the template method at CDF*, Phys. Rev. D **83** (2011) 111101, arXiv:1105.0192 [hep-ex].

[10] CDF Collaboration, *Measurement of the top quark mass in the all-hadronic mode at CDF*, Phys. Lett. B **714** (2012) 24, arXiv:1112.4891 [hep-ex].

[11] CDF Collaboration, *Top-quark mass measurement in events with jets and missing transverse energy using the full CDF data set*, Phys. Rev. D **88** (2013) 011101, arXiv:1305.3339 [hep-ex].

[12] D0 Collaboration, *Precise measurement of the top-quark mass from lepton+jets events at D0*, Phys. Rev. D **84** (2011) 032004, arXiv:1105.6287 [hep-ex].

[13] D0 Collaboration, *Measurement of the top-quark mass in proton-antiproton collisions using events with two leptons*, Phys. Rev. D **86** (2012) 051103, arXiv:1201.5172 [hep-ex].

[14] ATLAS Collaboration, *Measurement of the Top Quark Mass from* $\sqrt{s} = 7$ TeV *ATLAS Data using a 3-dimensional Template Fit*, conference note ATLAS-CONF-2013-046, 2013. http://cdsweb.cern.ch/record/1547327.

[15] ATLAS Collaboration, *Measurement of the Top Quark Mass in Dileptonic Top Quark Pair Decays with* $\sqrt{s} = 7$ TeV *ATLAS Data*, conference note ATLAS-CONF-2013-077, 2013. http://cds.cern.ch/record/1562935.

[16] CMS Collaboration, *Measurement of the top-quark mass in* $t\bar{t}$ *events with lepton+jets final states in pp collisions at* $\sqrt{s} = 7$ TeV, JHEP **12** (2012) 105, arXiv:1209.2319 [hep-ex].

[17] CMS Collaboration, *Measurement of the top-quark mass in $t\bar{t}$ events with dilepton final states in pp collisions at* $\sqrt{s} = 7$ TeV, Eur. Phys. J. **C72** (2012) 2202, arXiv:1209.2393 [hep-ex].

[18] CMS Collaboration, *Measurement of the top quark mass in the all-jets final states*, arXiv:1307.4617 [hep-ex]. Accepted by Eur. Phys. J. C.

[19] A. Buckley et al., *General-purpose event generators for LHC physics*, Phys. Rept. **504** (2011) 145, arXiv:1101.2599 [hep-ph].

[20] A. Juste et al., *Determination of the top quark mass circa 2013: methods, subtleties, perspectives*, arXiv:1310.0799 [hep-ph].

[21] L. Lyons, D. Gibaut and P. Clifford, *How to combine correlated estimates of a single physical quantity*, Nucl. Instrum. Meth. **A270** (1988) 110.

[22] A. Valassi, *Combining correlated measurements of several different physical quantities*, Nucl. Instrum. Meth. **A500** (2003) 391.

[23] R. Nisius, *A ROOT class to combine a number of correlated estimates of one or more observables using the Best Linear Unbiased Estimate method*, software version 1.8.0. http://blue.hepforge.org/.

[24] CDF Collaboration, *Topology of three-jet events in $p\bar{p}$ collisions at* $\sqrt{s} = 1.8$ TeV, Phys. Rev. D **45** (1992) 1448.

[25] G.C. Blazey et al. in *Proceedings of the Workshop on QCD and Weak Boson Physics in Run II (Fermilab, Batavia, 2000)*. FERMILAB-PUB-00-297, 2000.

[26] W. Lampl et al., *Calorimeter Clustering Algorithms: Description and Performance*, public note ATL-LARG-PUB-2008-002, 2008. http://cds.cern.ch/record/1099735.

[27] ATLAS Collaboration, *Jet energy measurement with the ATLAS detector in proton-proton collisions at* $\sqrt{s} = 7$ TeV, Eur. Phys. J. **C73** (2013) 2304, arXiv:1112.6426 [hep-ex].

[28] ATLAS Collaboration, *Jet energy scale and its systematic uncertainty in $p\bar{p}$ collisions at* $\sqrt{s} = 7$ TeV *with ATLAS 2011 data*, conference note ATLAS-CONF-2013-004, 2013. http://cdsweb.cern.ch/record/1509552.

[29] M. Cacciari, G.P. Salam and G. Soyez, *The Anti-k_t jet clustering algorithm*, JHEP **0804** (2008) 063, arXiv:0802.1189 [hep-ph].

[30] CMS Collaboration, *Commissioning of the Particle-Flow Reconstruction in Minimum-Bias and Jet Events from pp Collisions at* 7 TeV, conference note no. CMS-PAS-PFT-10-002, (2010). http://cdsweb.cern.ch/record/1279341.

[31] A. Bhatti et al., *Determination of the Jet Energy Scale at the Collider Detector at Fermilab*, Nucl. Instrum. Methods in Phys. Res. Sect. A **566** (2006) 375, arXiv:hep-ex/0510047 [hep-ex].

[32] D0 Collaboration, *Determination of the Absolute jet Energy Scale in the DØ Calorimeters*, Nucl. Instrum. Methods in Phys. Res. Sect. A **424** (1999) 352, arXiv:hep-ex/9805009 [hep-ex].

[33] D0 Collaboration, *Jet energy scale determination in the D0 experiment*, arXiv:1312.6873 [hep-ex]. Submitted to Nucl. Instrum. Meth.

[34] CMS Collaboration, *Determination of Jet Energy Calibration and Transverse Momentum Resolution in CMS*, JINST. **6** (2011) P11002, arXiv:1107.4277 [hep-ex].

[35] CMS Collaboration, *Jet Energy Scale performance in 2011*, CMS detector performance note CMS-DP-2012-006, 2012. https://cds.cern.ch/record/1454659.

[36] T. Sjostrand, S. Mrenna and P. Skands, *Pythia 6.4 physics and manual*, JHEP **05** (2006) 026, arXiv:hep-ph/0603175 [hep-ph].

[37] CDF Collaboration, *Charged jet evolution and the underlying event in $p\bar{p}$ collisions at 1.8 TeV*, Phys. Rev. D **65** (2002) 092002.

[38] M. Mangano, et al., *ALPGEN, a Generator for Hard Multiparton Processes in Hadronic Collisions*, JHEP **07** (2003) 001, arXiv:hep-ex/0206293 [hep-ex].

[39] CDF and D0 Collaborations, *Combination of the top-quark mass measurements from the Tevatron collider*, Phys. Rev. D **86** (2012) 092003, arXiv:1207.1069 [hep-ex].

[40] M. Mangano, M. Moretti and F. Piccinini, *Matching matrix elements and shower evolution for top-pair production in hadronic collisions*, JHEP **01** (2007) 013, arXiv:hep-ph/0611129 [hep-ph].

[41] S. Frixione, P. Nason and C. Oleari, *Matching NLO QCD computations with parton shower simulations: the POWHEG method*, JHEP **11** (2007) 070, arXiv:0709.2092 [hep-ph].

[42] P. Skands, *Tuning Monte Carlo Generators: The Perugia Tunes*, Phys. Rev. D **82** (2010) 074018, arXiv:1005.3457 [hep-ph].

[43] J. Alwall et al., *MadGraph 5: going beyond*, JHEP **06** (2011) 128, arXiv:1106.0522 [hep-ph].

[44] R. Field, *Early LHC Underlying Event Data - Findings and Surprises*, arXiv:1010.3558 [hep-ph].

[45] The Z2 tune is identical to the Z1 tune described in [44] except that Z2 uses the CTEQ6L PDF while Z1 uses CTEQ5L.

[46] CTEQ Collaboration, H.L. Lai et al., *Global QCD analysis of parton structure of the nucleon: CTEQ5 parton distributions*, Eur. Phys. J. **C12** (2000) 375–392, arXiv:hep-ph/9903282 [hep-ph].

[47] J.Pumplin et al., *New Generation of Parton Distribution with Uncertainties from Global QCD Analysis*, JHEP **0207** (2002) 012, arXiv:hep-ph/0201195 [hep-ph].

[48] H. Lai et al., *New parton distributions for collider physics*, Phys. Rev. D **82** (2010) 074024, arXiv:1007.2241 [hep-ph].

[49] P. Nadolsky et al., *Implications of CTEQ global analysis for collider observables*, Phys. Rev. D **78** (2008) 013004, arXiv:0802.0007 [hep-ph].

[50] CDF Collaboration, *Measurements of the top-quark mass using charged particle tracking*, Phys. Rev. D **81** (2010) 032002, arXiv:0910.0969 [hep-ex].

[51] CDF Collaboration, *Measurement of the top quark mass in the lepton+jets channel using the lepton transverse momentum*, Phys. Lett. B **698** (2011) 371, arXiv:1101.4926 [hep-ex].

[52] K. Cranmer, *Kernel estimation in high-energy physics*, Comput. Phys. Commun. **136** (2001) 198, arXiv:hep-ex/0011057 [hep-ex].

[53] D0 Collaboration, *Measurement of the top quark mass in the dilepton channel*, Phys. Rev. D **60** (1999) 052001, arXiv:hep-ex/9808029 [hep-ex].

[54] CDF Collaboration, *Measurement of the top quark mass using template methods on dilepton events in $p\bar{p}$ collisions at $\sqrt{s}$ = 1.96 TeV*, Phys. Rev. D **73** (2006) 112006, arXiv:hep-ex/0602008 [hep-ex].

[55] CDF Collaboration, *Top quark mass measurement using the template method in the lepton+jets channel at CDF II*, Phys. Rev. D **73** (2006) 032003, arXiv:hep-ex/0510048 [hep-ex].

[56] D0 Collaboration, *Measurement of the top quark mass in the lepton+jets final state with the matrix element method*, Phys. Rev. D **74** (2006) 092005, arXiv:hep-ex/0609053 [hep-ex].

[57] T. Aaltonen et al., *Improved b-jet Energy Correction for $H \to b\bar{b}$ Searches at CDF*, arXiv:1107.3026 [hep-ex].

[58] D0 Collaboration, *A precision measurement of the mass of the top quark*, Nature **429** (2004) 638, arXiv:hep-ex/0406031 [hep-ex].

[59] D0 Collaboration, *Precise measurement of the top quark mass from lepton+jets events at D0*, Phys. Rev. Lett. **101** (2008) 182001, arXiv:0807.2141 [hep-ex].

[60] D0 Collaboration, *Combination of the D0 the top quark mass measurements*, conference note D0 Note 5900, 2009.

[61] D0 Collaboration, *Measurement of the top quark mass in final states with two leptons*, Phys. Rev. D **80** (2009) 092006, arXiv:0904.3195 [hep-ex].

[62] DELPHI Collaboration, *Measurement of the Mass and Width of the W Boson in e^+e^- Collisions at $\sqrt{s}$ = 161 GeV-209 GeV*, Eur. Phys. J. **C55** (2008) 1–38, arXiv:0803.2534 [hep-ex].

[63] CMS Collaboration, *Measurement of the mass of the $t\bar{t}$ system by kinematic endpoints in pp collisions at $\sqrt{s}$ = 7 TeV*, Eur. Phys. J. C. **73** (2013) 2494, arXiv:1304.5783 [hep-ex].

[64] CMS Collaboration, *Measurement of the top-quark mass using the B-hadron lifetime technique*, conference note CMS-PAS-TOP-12-030, 2013. https://cds.cern.ch/record/1563140.

[65] ATLAS Collaboration, *Jet energy measurement for inclusive jets and b-quark induced jets*, conference note ATLAS-CONF-2013-002, 2013. http://cdsweb.cern.ch/record/1504739.

[66] G. Corcella et al., *HERWIG 6.5: an event generator for Hadron Emission Reactions With Interfering Gluons (including supersymmetric processes)*, JHEP **01** (2001) 010, arXiv:hep-ph/0011363 [hep-ph].

[67] W.-M. Yao et al., *Review of Particle Physics*, Journal of Physics G **33** (2006) 1+. http://pdg.lbl.gov.

[68] M. Bowler, *e^+e^- Production of Heavy Quarks in the String Model*, Z. Phys. C **11** (1981) 169.

[69] SLD Collaboration, *Precise measurement of the b quark fragmentation function in Z^0 boson decays*, Phys. Rev. Lett. **84** (2000) 4300, arXiv:hep-ex/9912058 [hep-ex].

[70] ALEPH Collaboration, *Study of the fragmentation of b quarks into B mesons at the Z peak*, Phys. Lett. B **512** (2001) 30, arXiv:hep-ex/0106051 [hep-ex].

[71] DELPHI Collaboration, *A Study of the b-Quark Fragmentation Function with the DELPHI Detector at LEP I*, conference note DELPHI-2002-069-CONF-603, 2002. https://cds.cern.ch/record/994376.

[72] OPAL Collaboration, *Inclusive analysis of the b quark fragmentation function in Z decays at LEP*, Eur. Phys. J. **C29** (2003) 463, arXiv:hep-ex/0210031 [hep-ex].

[73] D0 Collaboration, *Precise Tuning of the b Fragmentation for the DØ Monte Carlo*, Fermilab Technical Memo No. 2425-E, 2006. http://lss.fnal.gov/archive/test-tm/2000/fermilab-tm-2425-e.pdf.

[74] J.M Butterworth, J.R. Forshaw and M.H. Seymour, *Multiparton interactions in photoproduction at HERA*, Z. Phys. **C72** (2006) 637, arXiv:hep-ph/9601371 [hep-ph].

[75] R. Field and R. Craig Group, *PYTHIA tune A, HERWIG, and JIMMY in Run 2 at CDF*, arXiv:hep-ph/0510198 [hep-ph].

[76] S. Frixione, B. Webber and P. Nason, *MC@NLO Generator version 3.4*, arXiv:hep-ph/0204244, hep-ph/0305252 [hep-ph].

[77] S. Frixione, P. Nason and B.R. Webber, *Matching NLO QCD and parton showers in heavy flavour production*, JHEP **08** (2003) 007, arXiv:hep-ph/0305252 [hep-ph].

[78] CDF Collaboration, *Top Quark Mass Measurement Using the Template method in the Lepton+Jets Channel at CDF II*, Phys. Rev. D **73** (2006) 032003, arXiv:hep-ex/0510048 [hep-ex].

[79] ATLAS Collaboration, *Measurement of $t\bar{t}$ production with a veto on additional central jet activity in pp collisions at $\sqrt{s}$ = 7 TeV using the ATLAS detector*, Eur. Phy. J. **C72** (2012) 2043, arXiv:1203.5015 [hep-ex].

[80] ATLAS Collaboration, *Monte Carlo generator comparisons to ATLAS measurements constraining QCD radiation in top anti-top final states*, public note ATL-PHYS-PUB-2013-005, 2013. https://cds.cern.ch/record/1532067.

[81] CMS Collaboration, *Measurement of jet multiplicity in di-leptonic top pair events*, conference note CMS-PAS-TOP-12-023, 2012. https://cds.cern.ch/record/1478672.

[82] P. Skands and D. Wicke, *Non-perturbative QCD effects and the top mass at the Tevatron*, Eur. Phys. J. **C52** (2007) 133–140, arXiv:hep-ph/0703081 [hep-ph].

[83] P. Skands, *The Perugia Tunes*, arXiv:0905.3418 [hep-ph].

[84] A. Martin, R. Roberts, W. Stirling, and R. Thorne, *Parton Distributions: A New Global Analysis*, Eur. Phys. J. C **4** (1998) 463, arXiv:hep-ph/9803445 [hep-ph].

[85] M. Botje et al., *The PDF4LHC Working Group Interim Recommendations*, arXiv:1101.0538 [physics.data-an].

[86] S. Dittmaier, et al., *Handbook of LHC Higgs Cross Sections: 2. Differential Distributions*, arXiv:1201.3084 [hep-ph].

[87] ATLAS Collaboration, *Jet energy resolution in proton-proton collisions at $\sqrt{s}$ = 7 TeV recorded in 2010 with the ATLAS detector*, Eur. Phy. J. **C3** (2013) 2306, arXiv:1210.6210 [hep-ex].

[88] ATLAS Collaboration, *Performance of missing transverse momentum reconstruction in proton-proton collisions at $\sqrt{s}$ = 7 TeV with ATLAS*, Eur. Phy. J. **C72** (2012) 1844, arXiv:1108.5602 [hep-ex].

[89] CMS Collaboration, *Missing transverse energy performance of the CMS detector*, JINST **6** (2011) P09001, arXiv:1106.5048 [hep-ex].

[90] CDF Collaboration, *Measurement of the $t\bar{t}$ production cross section in $p\bar{p}$ collisions at $\sqrt{s}$ = 1.96 TeV using lepton + jets events with secondary vertex b-tagging*, Phys. Rev. D **71** (2005) 052003, arXiv:hep-ex/0410041 [hep-ex].

[91] ATLAS Collaboration, *Measuring the mistag rate with 5 fb^{-1} of data from the ATLAS detector*, conference note ATLAS-CONF-2012-040, 2012. http://cds.cern.ch/record/1435194.

[92] ATLAS Collaboration, *Measuring the b-tag efficiency in a $t\bar{t}$ sample with 4.7 fb^{-1} of data from the ATLAS detector*, conference note ATLAS-CONF-2012-097, 2012. http://cds.cern.ch/record/1460443.

[93] ATLAS Collaboration, *Measuring the b-tag efficiency in a sample of jets containing muons with 5 fb^{-1} of data from the ATLAS detector*, conference note ATLAS-CONF-2012-043, 2012. http://cds.cern.ch/record/1435197.

[94] CMS Collaboration, *Commissioning of b-jet identification with pp collisions at $\sqrt{s}$ = 7 TeV*, conference note CMS-PAS-BTV-10-001, 2010. http://cdsweb.cern.ch/record/1279144/.

[95] D0 Collaboration, *b-Jet Identification in the D0 Experiment*, Nucl. Instrum. Meth. **A620** (2010) 490–517, arXiv:1002.4224 [hep-ex].

[96] ATLAS Collaboration, *Electron performance measurements with the ATLAS detector using the 2010 LHC proton-proton collision data*, Eur. Phys. J **C72** (2012) 1909, arXiv:1110.3174v2 [hep-ph].

[97] ATLAS Collaboration, *Muon Momentum Resolution in First Pass Reconstruction of pp Collision Data Recorded by ATLAS in 2010*, conference note ATLAS-CONF-2011-046, 2011. https://cdsweb.cern.ch/record/1338575.

[98] CMS Collaboration, *Performance of CMS muon reconstruction in pp collision events at $\sqrt{s}$ = 7 TeV*, JINST **7** (2012) P10002, arXiv:1206.4071v1 [hep-ph].

[99] A. Valassi, R. Chierici, *Information and treatment of unknown correlations in the combination of measurements using the BLUE method*, arXiv:1307.4003 [physics.data-an].

[100] R. Nisius, *On the combination of correlated estimates of physics observables*, arXiv:1402.4016 [physics.data-an].

[101] CMS Collaborations, *Combination of the CMS measurements of the top quark mass based on data recorded between 2010 and 2012*, conference note CMS-PAS-TOP-13-002, 2013. http://cds.cern.ch/record/1599576.